



Univariate and multivariate forecasting of the electricity futures curve using Dynamic Recurrent Neural Networks

Oleksandr Castello^{a,*} , Marina Resta^b 

^a Department of Economics, Cà Foscari University of Venice, Sestiere Cannaregio 873, Venice, 30121, Italy

^b Department of Economics and Business Studies, University of Genoa, Via Vivaldi 5, Genoa, 16126, Italy

HIGHLIGHTS

- We developed a Machine Learning approach to predict the term structure of electricity futures prices.
- The framework is tested for univariate and multivariate forecasting using real-world power data, showing cutting-edge results.
- The role of various exogenous factors is assessed.
- Forecasts are made on both stable and extremely volatile test sets to thoroughly evaluate the models' predictive power.
- A comparative study with popular statistical and ML methods was carried out.

ARTICLE INFO

Keywords:

Dynamic Recurrent Neural Networks
Electricity futures curve prediction
Futures prices term structure
LSTM-NN models
NAR-NN
NARX-NN

ABSTRACT

In recent years international power markets have witnessed high uncertainty and extraordinary volatility which, given the inherent complexity of the market, has made the Electricity Price Forecasting (EPF) process increasingly difficult. Therefore the development of a proper forecasting framework suitable for both stable and volatile periods has assumed an increasing importance for market players and policymakers in both strategic planning and risk management. At present, the majority of the studies on electricity price forecasting focused on the analysis of spot markets, neglecting the importance of derivative price modeling to mitigate the risks induced by market downturns and turmoil. Our study nests within this research stream and analyzes the potential of a set of state-of-the-art Machine Learning (ML) models for the prediction of the term structure of electricity futures prices. The objective is to define an ML-based framework capable of ensuring high predictive performance of the term structure during both stable and extremely turbulent conditions. In this regard we examined the predictive capabilities of a variety of Dynamic Recurrent Neural Networks (DRNNs) including: Nonlinear Autoregressive Neural Networks (NAR-NNs), NAR with Exogenous Inputs (NARX-NNs), Long Short-Term Memory (LSTM-NNs), Stacked Long Short-Term Memory (ST-LSTM-NNs), Bidirectional Long Short-Term Memory (BI-LSTM-NNs) and Encoder–Decoder Long Short-Term Memory Neural Networks (ED-LSTM-NNs). The models were applied to both low fluctuating and volatile sets of daily futures prices of the European Energy Exchange (EEX) for univariate as well as multivariate forecasting. Additionally, we compared this set of networks to baseline models commonly used in the EPF literature, including classical statistical and ML methods. Empirical results highlighted that DRNN models predictions are consistent with futures prices trends observed under different market regimes and outperform the competitors' performance. Overall, main outcomes of the study may be summarized as follows: LSTM-based models seem to have the highest predictive power, with robust performance under various conditions. In detail the Multivariate BI-LSTM-NN performs better under quiet market conditions ensuring an accuracy level of 98.11 %, while the Univariate ED-LSTM-NN ensures superior predictive performance in presence of turmoil, achieving a 95.33 % accuracy.

* Corresponding author.

Email address: oleksandr.castello@unive.it (O. Castello).

<https://doi.org/10.1016/j.apenergy.2025.126082>

Received 24 August 2024; Received in revised form 11 March 2025; Accepted 6 May 2025

Available online 28 May 2025

0306-2619/© 2025 Published by Elsevier Ltd.

Nomenclature

ADAM	Adaptive Moment Estimation	M-SVR	Multivariate Support Vector Regression
AR	Autoregressive	MAPE	Mean Absolute Percentage Error
ARX	Autoregressive with Exogenous Regressors	MEFPP	Multivariate Electricity Futures Price Prediction Process
BI-LSTM-NN	Bidirectional Long Short-Term Memory Neural Network	ML	Machine Learning
BM	Baseline Models	MLP	Multilayer Perceptron
BP-NN	Back-Propagation Neural Network	NAR-NN	Nonlinear Autoregressive Neural Network
CO ₂	Carbon Emission Certificates	NARX-NN	Nonlinear Autoregressive Neural Network with Exogenous Inputs
DRNN	Dynamic Recurrent Neural Network	NG	Natural Gas
ED-LSTM-NN	Encoder–Decoder Long Short-Term Memory Neural Network	PCA	Principal Component Analysis
EEX	European Energy Exchange	RBF-NN	Radial Basis Function Neural Network
EPF	Electricity Price Forecasting	RNN	Recurrent Neural Network
EU-ETS	European Emissions Trading System	RMSFE	Root Mean Squared Forecasting Error
EU	European Union	SARIMA	Seasonal Autoregressive Integrated Moving Average
FF-NN	Feed-Forward Neural Network	SARIMAX	Seasonal Autoregressive Integrated Moving Average with Exogenous Regressors
HLN	Harvey-Leybourne-Newbold	ST-LSTM-NN	Stacked Long Short-Term Memory Neural Network
IW-NN	Improved Wavelet Neural Network	SVR	Support Vector Regression
JB	Jarque–Bera	TTF	Title Transfer Facility
LMBP	Levenberg–Marquardt Backpropagation	U-BI-LSTM-NN	Univariate Bidirectional Long Short-Term Memory Neural Network
LSTM-NN	Long Short-Term Memory Neural Network	U-ED-LSTM-NN	Univariate Encoder–Decoder Long Short-Term Memory Neural Network
M-BI-LSTM-NN	Multivariate Bidirectional Long Short-Term Memory Neural Network	U-LSTM-NN	Univariate Long Short-Term Memory Neural Network
M-ED-LSTM-NN	Multivariate Encoder–Decoder Long Short-Term Memory Neural Network	U-MLP	Univariate Multilayer Perceptron
M-LSTM-NN	Multivariate Long Short-Term Memory Neural Network	U-ST-LSTM-NN	Univariate Stacked Long Short-Term Memory Neural Network
M-MLP	Multivariate Multilayer Perceptron	U-SVR	Univariate Support Vector Regression
M-ST-LSTM-NN	Multivariate Stacked Long Short-Term Memory Neural Network	UEFPP	Univariate Electricity Futures Price Prediction Process

1. Introduction

Electricity is an essential source of energy in modern societies, playing a pivotal role in powering various segments of the economy such as the residential, commercial, industrial, and transport sectors. In this respect, changes in either the prices or the availability of this commodity can exert deep, beneficial as well as potentially devastating, knock-on effects on the social and economic fabric, affecting the development prospects of countries.

Exogenous events, such as the climate change, green economy policies, deregulation, as well as the geopolitical crises in more recent times, can have a significant impact on international electricity markets, increasing uncertainty and price volatility, with sudden spikes and drops in price levels [45,120]. An evidence in this sense is provided by considering the period from mid-2021 to the end of 2022, when price dynamics have experienced rapid growth and unprecedented highs in terms of both price levels and volatility [129]. The primary reason for this sensitivity to exogenous events lies in the specific features that make electricity a *unicum* with respect to other energy commodities, namely, non-storability, i.e. the impossibility of storing electricity in sufficient quantities at a reasonable price and the presence of inelastic demand, that is the absence of significant and quick demand adjustments to price/supply changes. These features are a source of complexity in managing the impact on prices of abrupt shifts in supply and demand. This, in turn, exposes market participants to significant risks in power prices.

In light of this, risk management plays a key role in mitigating the effects of an excessive exposure to market price volatility and futures contracts are probably the most widespread financial instruments used to hedge positions.

Electricity futures contracts traded on financial markets can have different delivery periods, ranging from a few days to weeks, a season, or

a whole year. Additionally, they are characterized by various maturities which span from short-term, in the case of day, weekend and week futures, to mid-long term as in the case of monthly, quarterly and yearly contracts. It is a common practice to analyze them as a whole, examining how the price evolves along the maturity spectrum, thus forming the so-called term structure of futures prices.

The term structure describes the relationship between the settlement prices of futures contracts and different expiration dates, with the futures curve being its graphical representation. Studying its evolution over time, on the one hand, gives an idea of the market supply and demand dynamics, as it is known that the curve incorporates practitioners' expectations about the market behavior [38], while on the other hand, it allows for the definition of properly structured investment and hedging strategies.

Setting aside speculative purposes, electricity futures contracts are used by the counterparties with the main goal of reducing their risk exposure: power producers, in particular, will take short positions on futures contracts to lock in a guaranteed price, thereby hedging against any downward movements in the spot price and decreasing the volatility of their revenues; consumers and power retailers, for their part, will take long positions and leverage the different delivery periods in contracts to buy/sell the good at a fixed price, thereby reducing the risk of encountering sudden price spikes. All this leads to greater stability in price and supply, with direct benefits to both the social fabric and the economy in terms of development and competitiveness. In this respect obtaining reliable forecasts of the futures curve dynamics and trends becomes of paramount importance in many scenarios and for different market players.

To date, the overwhelming majority of research studies have focused on power spot price modeling and forecasting. Extensive reviews of the state-of-the-art can be found in [23,32,39,101,143]. According

to [37] the most widely used models are those belonging to the class of fundamental methods [27,35,46,61,62,83,102,113,128] that model electricity price dynamics assuming the influence of fundamental drivers (e.g. demand, loads, weather conditions), and reduced-form methods [7,18,30,31,51,89,100,105,139] which explain price dynamics by investigating main features like seasonal volatility, spikes, time-varying mean reversion and correlations between commodity prices. Furthermore, a plenty of works focused on statistical/econometric methods [24,72,91,112,116,125,131,149,153] to develop modeling frameworks based on endogenous historical price values and/or exogenous variable values, as well as on probabilistic techniques [58,70,98,110,152] that model spot prices by quantifying prediction uncertainty, and hybrid approaches [12,25,63,73,93,145,147,148] which combine techniques from two or more of the groups listed above.

Moreover, in light of the features characterizing electricity price dynamics, in the last decades Machine Learning (ML) models have gained increasing attention: a significant portion of publications in the EPF field make use of these methods as they have shown excellent modeling performances due to their capability to handle unstable nonlinear data dynamics [53]. Unlike the other approaches, ML techniques, on the one hand, don't make assumptions about the functional form or statistical properties of the data set under examination, while on the other hand, they rely on nonlinear optimization techniques. These features make them overall more effective, accurate and hence popular for predictive purposes. In this regard, various techniques combining learning, evolution and fuzziness have been developed [135]. The result is a plethora of approaches capable of adapting to complex dynamic systems and achieving accurate power price predictions [57,84,104,107,121,127,142,151]. Readers can refer to the surveys in [74,99,135] for a comprehensive study of the aforementioned classes of models.

However, research about predicting futures prices dynamics is relatively more limited and less diversified. Most of the literature, in fact, focuses mainly on modeling price dynamics or on deriving futures prices from spot prices with various pricing techniques based on stochastic processes, rather than on direct futures curve prediction. To make some examples, likewise in the spot market, most commonly used methods in the research literature include reduced-form methods as well as structural methods. Reduced-form methods, in turn, include a wide spectrum of modeling approaches ranging from factor/term structure methods based on stochastic processes [13,15,22,39,40,44,69,138], to regime-switching frameworks [86], stochastic partial differential equation models [11,14,87], volatility models [55] and jump/diffusion models [21,49,95]; while structural methods include equilibrium-based models [3,60], econometric approaches [65,108] as well as merit-order frameworks [43]. With respect to ML techniques, their predictive abilities within the electricity futures market haven't been extensively analyzed as done for spot markets. To the best of the authors' knowledge, in fact, there are no published papers exploring the potential of computational intelligence methods to directly forecast electricity futures prices and/or the whole term structure, with some notable exceptions including: [144] who discussed a framework based on Principal Component Analysis (PCA) and Improved Wavelet Neural Networks (IW-NN) with multiple input variables (power futures and average spot price, consumption, production, demand, weekly reservoir generation) for daily predictions in the Nord Pool market; [146] who suggested a Radial Basis Function Neural Network (RBF-NN) for the pointwise forecasting within the Nordic electricity market comparing it to a simple Back-Propagation Neural Network (BP-NN), and [96] who developed a simple Feed-Forward Neural Network (FF-NN) containing several external variables (consumption, generation, prices and weather data) for monthly price forecasting in the Iberian electricity market.

Although the above mentioned NN models are endowed with greater robustness and nonlinear mapping capabilities compared to traditional methods, their main drawback lies in the lower ability to examine the

relationship between data and time and hence to capture temporal correlations in sequential/time series data due to the lack of dynamic memory [54,133]. Therefore, it is the authors' opinion that there is enough room to explore more sophisticated NN architectures capable of managing not only nonlinearity, but also capturing and leveraging internal time dependencies of historical datasets, thus representing an invaluable tool to achieve accurate forecasts.

An additional "limitation" of the cited literature is the focus on price dynamics predictions of single futures contracts, thereby neglecting the modeling of the whole term structure. This gap needs to be addressed in state-of-the-art research papers, given the paramount importance of the term structure for production, operation, investment and risk management strategies outlined in the previous lines.

Based on the above premises as well as on the belief that the capabilities of ML models haven't yet been fully unraveled in this field, this study develops a framework based on Dynamic Recurrent Neural Networks (DRNNs) to tackle the issue of predicting the electricity futures prices term structure dynamics. These models have achieved cutting-edge results in various fields such as economics [5,10,17,78,80,97,106,111,118,126], physics [41,82,123,130,141], medicine [2,33,88,109,136] and finance [6,34,71,81,90,115,140], gaining significant success also within energy commodities markets [1,9,29,119,132,134,150] due to their ability to manage complex nonlinear problems involving temporal dependencies within sequential and time series data, as well as noisy and chaotic datasets.

DRNNs can represent a more robust, flexible and data-driven alternative to conventional methods, which often struggle to adapt to market changes requiring frequent parameter recalibration or new model specifications, due to their reliance on (i) predefined economic/financial/stochastic assumptions about price formation and market behavior, and (ii) the Markovian properties or simplified structures that limit memory depth. By leveraging flexible function approximation, temporal feature extraction, adaptive learning, and deep recurrent architectures, DRNNs learn temporal dependencies and nonlinear relationships directly from data, and can thus detect and dynamically adapt to structural shifts, regime changes, and extreme price fluctuations without relying on predefined functional forms or imposing rigid assumptions on underlying processes and distributions. As a result, DRNNs seem particularly well-suited for modeling intricate dynamics, extreme fluctuations, and uncovering hidden structural patterns that traditional models often overlook.

Overall, these properties turn out to be of crucial importance in the electricity futures market since electricity price data are characterized by high volatility, non-linearity and non-stationarity.

We therefore examined a set of DRNNs including: the Nonlinear Autoregressive Neural Network (NAR-NN), Nonlinear Autoregressive Neural Network with Exogenous Inputs (NARX-NN), Long Short-Term Memory Neural Network (LSTM-NN), Stacked Long Short-Term Memory Neural Network (ST-LSTM-NN), Bidirectional Long Short-Term Memory Neural Network (BI-LSTM-NN) and Encoder-Decoder Long Short-Term Memory Neural Network (ED-LSTM-NN) for day-ahead predictions of the electricity futures curve. We explored the models ability in both univariate and multivariate forecasting. At first, we assessed the potential of the models to obtain robust electricity futures curves predictions considering only endogenous past values, i.e. using the autoregressive dynamics of the target series that form the futures curve. In a second moment, we tested whether embedding exogenous factors can lead to improvements in the models' forecasting power. To such aim, we incorporated into the neural models the more closely related covariates such as Natural Gas (NG) and Coal futures prices as well as Carbon Emission Certificates (CO₂) spot prices since they represent important electricity generation costs [8] that significantly influence the dynamics of electricity futures prices.

Additionally, the overall adequacy of the forecasting framework was assessed under both steady and critical market conditions. To this end, we collected data spanning March 2017 to September 2023, ensuring the

inclusion of periods of relevant uncertainty and volatility (e.g. the Covid-19 pandemic and the 2021–2023 global energy crises), and examined the framework across two contrasting time spans: one more stable with low variations in the price levels, and another marked by an extreme variety of behaviors, and generally, by very high volatility.

Finally, to fully evaluate the robustness and effectiveness of the networks' predictive performances, we compared the proposed framework against a set of well-established baseline models commonly used in the EPF literature, that is classical statistical (i.e. ARIMA-based models) and ML (i.e. Multilayer Perceptron, Support Vector Regression) methods. In order to ensure homogeneity and comparability of the results, all the baseline models were used in the univariate and multivariate settings as well.

Overall, this work contributes to the existing literature towards many directions that are summarized as follows: (i) we focused on the power futures market, stressing the importance of derivatives for risk hedging purposes; (ii) we run day-ahead forecasts of electricity futures prices term structure with state-of-the-art Dynamic Recurrent Neural Networks; (iii) we addressed some issues raised in [74] by comparing different complex Deep Learning (DL) architectures to show their performance with respect to each other, and by using relatively long test sets to ensure meaningful conclusions; (iv) we performed both univariate and multivariate predictions and stress-tested the framework under various market regimes; (v) we extended the idea behind fundamental models to DRNNs and incorporated different time-dependent exogenous input variables to enhance neural networks' predictive abilities; (vi) we tested the ML-based framework using real market data from the leading and most liquid energy exchange worldwide, i.e. The European Energy Exchange (EEX); and finally (vii) by also considering periods characterized by significant uncertainty we contributed to evaluating the predictability of energy commodities futures prices under extreme market conditions.

The remainder of the paper is organized as follows. Section 2 discusses the DRNN models in use; Section 3 analyzes the data set; Section 4 presents the empirical findings and discusses the main results; Section 5 concludes.

2. Recurrent Neural Networks-based models

Recurrent Neural Networks (RNNs) are a class of deep neural networks designed for modeling either sequential data or time series for predictions where past information plays a pivotal role. Key features of RNNs include feedback loop-based architecture and memory mechanisms which enable the network to learn features as well as short-term and/or long-term dependencies of the data, storing the relevant information and employing this knowledge to generate future outputs of the data sequence.

In this section we present and discuss six types of RNNs that have gained wide success for univariate and multivariate forecasting of time-series, namely the Nonlinear Autoregressive (NAR-NNs), Nonlinear Autoregressive with Exogenous Inputs (NARX-NNs), Long Short-Term Memory (LSTM-NNs), Stacked Long Short-Term Memory (ST-LSTM-NNs), Bidirectional Long Short-Term Memory (BI-LSTM-NNs) as well as Encoder–Decoder Long Short-Term Memory Neural Networks (ED-LSTM-NNs).

2.1. Nonlinear Autoregressive Neural Networks

The Nonlinear Autoregressive Neural Network (NAR-NN) and the Nonlinear Autoregressive Neural Network with Exogenous variables (NARX-NN) are conceived as a nonlinear generalization of the classical linear Autoregressive (AR) model, aimed at managing nonlinear processes [4].

Given the univariate time series $\{x_t\}$, the NAR-NN predicts the future value at time t based on the d past endogenous values (feedback delays)

used as regressors:

$$x_t = f(x_{t-1}, x_{t-2}, \dots, x_{t-d}), \quad (1)$$

where $f(\cdot)$ is a nonlinear transfer function as it will be discussed later in this section, while x_{t-j} ($j = 1, \dots, d$) are the endogenous lagged input signals.

The NARX-NN model is a modified version of the above NAR-NN and it takes advantage of the information incorporated into exogenous inputs. The NARX-NN, in fact, predicts the future value of the univariate series $\{x_t\}$ at time t using both the d past endogenous values of the series and the h lagged values of the exogenous series $\{y_t\}$:

$$x_t = g(x_{t-1}, x_{t-2}, \dots, x_{t-d}, y_{t-1}, y_{t-2}, \dots, y_{t-h}), \quad (2)$$

where x_{t-j} ($j = 1, \dots, d$) is the same as in 1, $g(\cdot)$ is a nonlinear transfer function, while y_{t-k} ($k = 1, \dots, h$) are the exogenous lagged input observations.

The NAR-NN and NARX-NN models are characterized by a fully connected Multilayer Feed-Forward Network [56] architecture in which interconnected information processing elements (neurons) are grouped into multiple sequential layers, namely:

- (a) the Input layer which propagates the input features to the adjacent Hidden layer;
- (b) one or more Hidden layer(s) between the Input and Output layers where the network tries to learn and recognize complex patterns in the data by means of nonlinear transformations of the inputs;
- (c) the final Output layer which leads to the predicted value x_t .

These networks also contain a re-feeding mechanism which allows the use of predicted values as inputs for future forecasts. The structure of the NAR-NN and NARX-NN models is given in Fig. 1.

The optimal topology, i.e. the optimal number of hidden layers, neurons, feedback delays and activation functions, depends on the problem domain. Usually it is identified following a trial and error approach by comparing different network configurations, and considering also the bias/variance tradeoff, i.e. the trade-off between the network's complexity and its ability to capture regularities in training data as well as generalize well to unseen data.

Once stated the topology, the network undergoes the training and learning processes in an Open Loop aimed at identifying the proper transfer function to form a correct mapping between lagged input series and target values making use only of observed historical data. In this phase, network parameters are calibrated by means of the back-propagation algorithm, such that the overall network error is minimized. Different learning algorithms can be used to optimize the loss function, the choice depends on factors like computational time, error goals, or the amount of training data, weights and biases. The Levenberg–Marquardt Backpropagation Algorithm (LMBP) [77,85] is one of the most widely used learning rules in NAR-NNs and NARX-NNs as it inherits the advantages of the steepest descent method (in terms of stability) and the Gauss–Newton algorithm (in terms of speed), hence ensuring robustness, fast convergence rate and quicker training speed [137]. In the end, the configuration that provides the best performance is chosen.

In this context, the transfer function $f(\cdot)$ for the NAR-NN given in (1) can be represented as follows:

$$x_t = \omega_0 + \sum_{i=1}^n \omega_i \Lambda \left(\alpha_{i,0} + \sum_{j=1}^d \alpha_{i,j} x_{t-j} \right), \quad (3)$$

while (2) for the NARX-NN turns into:

$$x_t = \omega_0 + \sum_{i=1}^n \omega_i \Lambda \left(\alpha_{i,0} + \sum_{j=1}^d \alpha_{i,j} x_{t-j} + \sum_{k=1}^h \gamma_{i,k} y_{t-k} \right). \quad (4)$$

Here, d and h are, respectively, the number of lagged endogenous ($x_{t-j}, j = 1, \dots, d$) and exogenous ($y_{t-k}, k = 1, \dots, h$) input units fed to

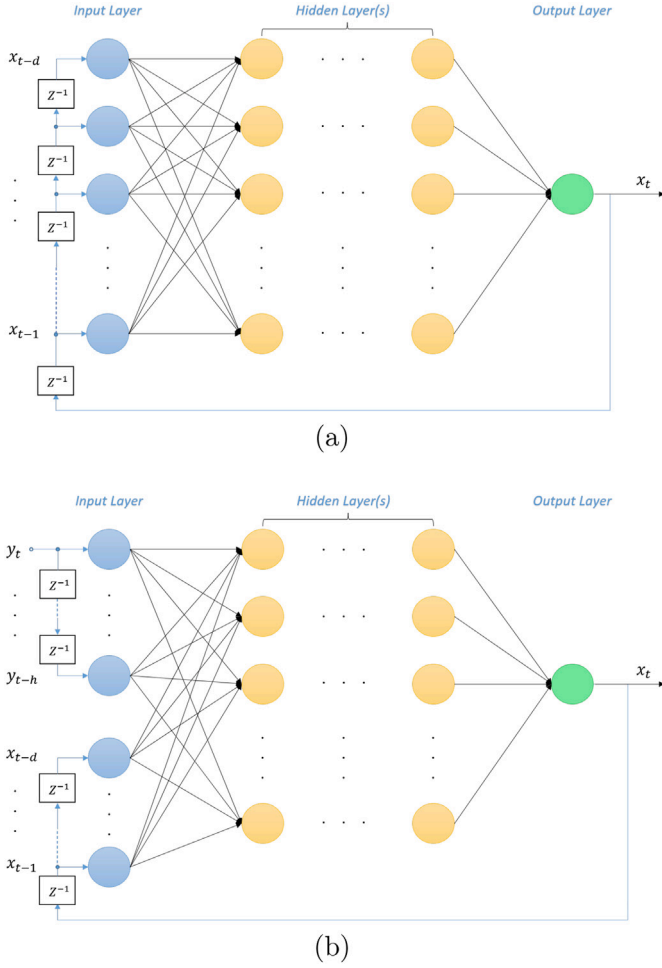


Fig. 1. Topology of the NAR-NN (a) and NARX-NN (b) models. Z^{-1} is the unit delay operator, blue circles are the neurons in the Input Layer, yellow circles represent nodes in the Hidden Layer(s), while the green node is the Output Layer.

each hidden neuron i ; $\Lambda(\cdot)$ is the activation function [124] (usually the sigmoid) that transforms the weighted sum of inputs and biases, managing either the activation or the deactivation of the networks neurons; $\alpha_{i,j}$ and $\gamma_{i,k}$ represent the neuron weight of the connection between the input units j , k and the hidden unit i ; ω_i is the weight of the connection between the hidden unit i and the output unit; finally $\alpha_{i,0}$ and ω_0 are the bias used to optimize the working point of the neurons in the hidden and output units respectively.

After the training, the optimal network is turned into a Closed Loop network and, leveraging internal feedback loops, it is used to execute one/multistep-ahead predictions (see Fig. 1) following an iterative approach: at each forecasting step the new predicted value is fed back towards the input layer through the re-feeding mechanism and is used to update the previous set of input lagged values to make new predictions in the next steps.

2.2. Long Short-Term Memory Network

The Long Short-Term Memory Neural Network (LSTM-NN) [52] is an RNN that can learn both short and long-term nonlinear dependencies in sequential data and retain relevant information over a long-term period. These features make it possible to overcome the RNNs' problem of vanishing/exploding gradients which hampers their ability to learn long data sequences.

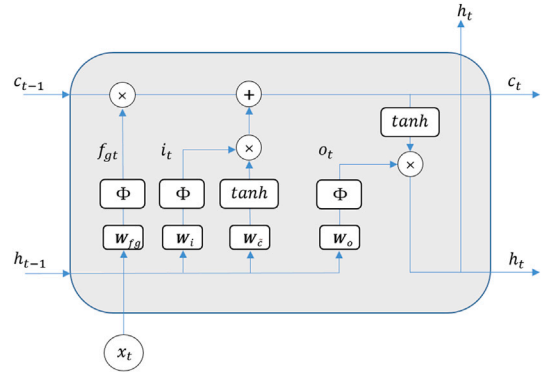


Fig. 2. Schematic representation of the LSTM memory unit. Here, c_{t-1} represents the cell state at time $t - 1$, and it is associated to the long-term memory; h_{t-1} is the hidden state at time $t - 1$, and it is associated to the short-term memory; x_t represents the current input vector; f_{gt} , i_t and o_t are the outputs associated to the Forget gate, Input gate and Output gate, respectively; Φ and \tanh identify, respectively, the logistic and the hyperbolic tangent activation functions; W_{fg} , W_i and W_o are the weight matrices used in the Forget, Input and Output gates, respectively; c_t and h_t represent the cell state and hidden state at current timestep t .

The LSTM-NN is characterized by a chain-like architecture with a linked sequence of repeating modules known as cells (or memory units), as illustrated in Fig. 2.

The key elements characterizing any LSTM cell are the cell state and the gating mechanisms that allow the creation of long temporal relationships. In particular, the cell state transports relevant stored information from earlier time steps through the entire sequence chain, acting like a *conveyor system*, and it is therefore interpreted as the long-term memory component. On the other hand, the gating mechanisms are responsible for deciding which information should be remembered and added to the cell state and which must be discarded, thus regulating the information flow within the LSTM unit.

In detail, each cell contains three types of gates, namely the *Forget gate*, the *Input gate* and the *Output gate*. The *Forget gate* determines whether the information from the previous time step has to be remembered and used in the cell state update process, or if it can be ignored: the gate receives the hidden state h_{t-1} and the current input value x_t as inputs and process them via the logistic function which returns values between 0 and 1. If the result is 0 then the information is completely discarded, otherwise it is retained. In a formal way the task performed by the gate can be expressed as follows:

$$f_{gt} = \Phi(W_{fg}h_{t-1} + W_{fg}x_t + b_{fg}) = \frac{1}{1 + e^{-(W_{fg}h_{t-1} + W_{fg}x_t + b_{fg})}}, \quad (5)$$

where $\Phi(\cdot)$ is the logistic activation function, while W_{fg} and b_{fg} represent the weight matrix and connection bias, respectively.

At this point, the *Input gate* determines which part of new information must be kept and used to update the current cell state c_t . In detail, the hidden state h_{t-1} and the current value x_t are processed via both the hyperbolic tangent activation function $\tanh(\eta) = (e^\eta - e^{-\eta}) / (e^\eta + e^{-\eta})^{-1}$, with $\eta = W_{\tilde{c}}h_{t-1} + W_{\tilde{c}}x_t + b_{\tilde{c}}$, and the logistic activation function $\Phi(\cdot)$ above described. The $\tanh(\cdot)$ function generates a vector of new candidate values \tilde{c}_t :

$$\tilde{c}_t = \tanh(W_{\tilde{c}}h_{t-1} + W_{\tilde{c}}x_t + b_{\tilde{c}}), \quad (6)$$

that can be used to update the cell state, while the sigmoid function creates a selector vector i_t that decides which information from the $\tanh(\cdot)$ output will be retained and used in the update process, according to the:

$$i_t = \Phi(W_i h_{t-1} + W_i x_t + b_i), \quad (7)$$

where W_i , b_i , $W_{\tilde{c}}$ and $b_{\tilde{c}}$ are as before.

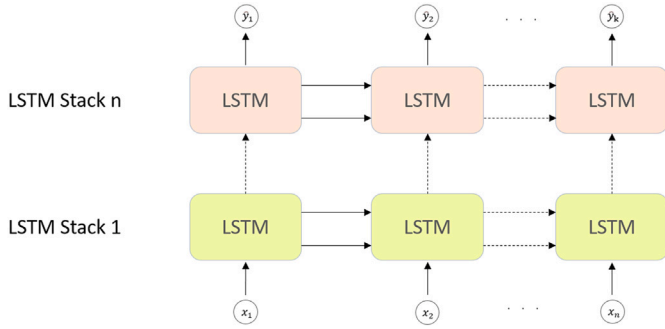


Fig. 3. Stacked LSTM Architecture. x_l ($l = 1, \dots, n$) represents the input data sequence; the yellow and pink cells are the LSTM memory units contained in the first and n -th mapping layers, respectively; \hat{y}_p ($p = 1, \dots, k$) is the networks output vector.

The cell state update is carried out by combining the results of (6) and (7) with the information retained from the previous cell state (c_{t-1}) given in (5):

$$c_t = f g_t \odot c_{t-1} + i \odot \tilde{c}_t, \quad (8)$$

where \odot is the Hadamard product.

Finally, the *Output gate* determines the value of the new hidden state h_t , i.e. the cell output, by filtering the updated cell state. This process consists of three main parts. At first, the *tanh* function is used on the newly updated cell state to obtain a candidate vector of outputs. Then, the output gate generates a selector vector by processing h_{t-1} and x_t through the function $\Phi(\cdot)$:

$$o_t = \Phi(\mathbf{W}_o h_{t-1} + \mathbf{W}_o x_t + b_o), \quad (9)$$

where o_t is the output value of the gate at time t , while \mathbf{W}_o and b_o are as before. Finally, the selector vector is combined with the candidate vector to determine which part of the information encoded in the updated cell state will be used as output of the memory cell:

$$h_t = o_t \odot \tanh(c_t), \quad (10)$$

where h_t is the LSTM cell output signal at time t .

2.3. Stacked LSTM model

Conventional LSTM neural networks are efficient at capturing correlation features or patterns in the data making use of a single hidden layer architecture only. However, [28,75] have shown that deep neural network architectures, i.e. those with multiple nonlinear mapping layers, are endowed with greater dependency learning capabilities, and as a consequence can achieve superior predictive performance. For this reason [47] developed deep LSTM-NNs, also known as Stacked LSTM-NNs (ST-LSTM-NN).

The ST-LSTM-NNs belong to the class of deep recurrent neural networks. As represented in Fig. 3, they contain several LSTM hidden layers stacked on top of each other to form a fully connected architecture.

Each layer is made up of multiple processing units, i.e. LSTM cells, and the output of each unit is not only propagated forward through time along the entire sequence chain, but it also works as an input to the cell in the successive hidden layer. Such an increased architectural complexity enables the network to build up higher level representations of the dataset, generalize better and, as a result, enhance the model's effectiveness in sequence prediction problems.

2.4. Bidirectional LSTM model

The Bidirectional LSTM neural network (BI-LSTM-NN) [48] represents an extension of the conventional LSTM-NN and it is designed to

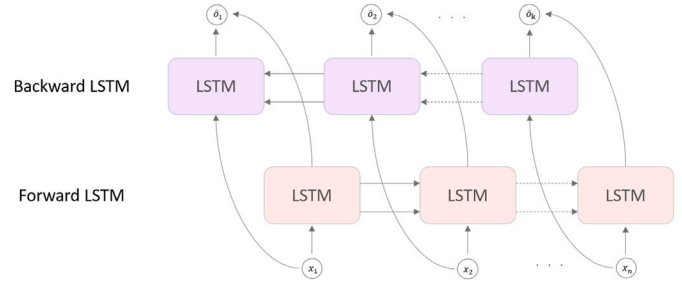


Fig. 4. Topology of the Bidirectional LSTM network. x_l ($l = 1, \dots, n$) represents the input data; the pink and violet cells are the LSTM units contained in the forward and backward hidden layers, respectively; \hat{o}_m ($m = 1, \dots, k$) is the networks output sequence.

incorporate the bidirectional concept [117] into LSTM-NN [68] in order to capture the short and long-term dependencies in bidirectional mode (backward and forward), thus contributing to boosting the overall accuracy of the original LSTM-NN for sequence learning tasks.

The core idea underlying the BI-LSTM-NNs is that the predicted output at every time step is not only the outcome of previous data information, but it also depends on the correlation with future information. Therefore, unlike unidirectional LSTM-NNs which make use only of previous contexts of the input to capture nonlinear patterns in the data, BI-LSTM networks process the data in both directions, that is forward (from past to future) and backward (from future to past), and include the preceding and succeeding input data sequences (i.e. both the preceding and succeeding correlations in the data) in the learning and training process to better identify the features/relationships in the data and thus enhance the network's predictive power.

To do this, the network relies on an architecture made up of two types of unidirectional hidden layers containing LSTM processing units, namely the Forward LSTM layer and the Backward LSTM layer as illustrated in Fig. 4.

The layers are chained together and connected to the same output layer. Each layer performs the operations on the input sequence as described in Section 2.2, but using a different flow direction. In particular, the Forward LSTM layer performs the operations following the forward direction of the data sequence thus exploiting the past context, while the Backward LSTM layer applies its operations on the reverse data sequence, hence exploiting the future context. This structure provides bidirectional short/long term memory to the network which allows it to involve the whole temporal horizon and implement not only the previous features but also use the upcoming information. The outputs produced by the network's forward (backward) layer(s) are not used as inputs to backward (forward) layer(s), but are combined by means of appropriate merging methods to generate the network's final output sequence.

2.5. Encoder-Decoder LSTM model

The Encoder–Decoder LSTM neural network [122] represents a combinatorial architecture based on the principles of Encoder–Decoder and LSTM networks used for solving the problem of mapping sequences to sequences characterized by variable dimensionality [20].

The network consists of three main components: the encoder and the decoder subnetworks and an intermediate fixed-length context vector. The encoder and decoder, in turn, are made up of one or multiple layers of LSTM cells representing their structural blocks as shown in Fig. 5.

The encoder's operating principle is based on the LSTM learning approach described in Section 2.2. Given a variable-length vector $x = (x_1, \dots, x_n)$ as the input sequence to the model, each LSTM unit in the encoder sequentially processes the incoming data, retains relevant features, and propagates the information forward through the sequence

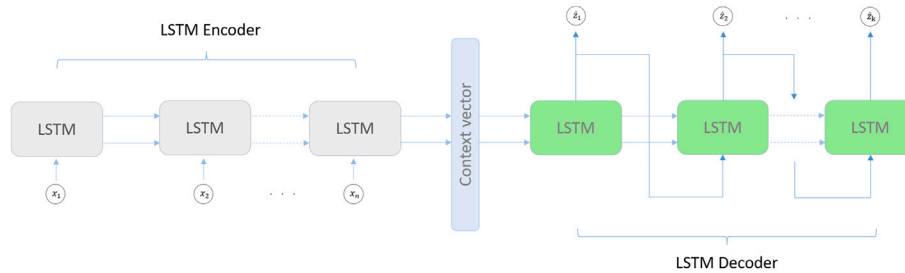


Fig. 5. Encoder-Decoder LSTM Architecture. The grey and green cells are the LSTM units constituting, respectively, the Encoder and Decoder networks; x_l ($l = 1, \dots, n$) represents the input vector to the Encoder, while z_q ($q = 1, \dots, k$) is the Decoders output sequence; finally, the intermediate level represents the Context vector.

chain. In the final step, the encoder squeezes and encodes the information into a fixed-length context vector, that is, the final cell (c) and hidden state (h) vectors, which in turn become the input to the decoder. At this stage, the decoder is initialised with the (c) and (h) vectors jointly with the last input value and starts the recursive generation of the output sequence $\hat{z} = (\hat{z}_1, \dots, \hat{z}_k)$ one time step at a time, using the obtained output as input for successive updates.

3. Data

Our dataset consists of daily closing prices of financially settled baseload monthly futures contracts from the Italian power market. The contracts are based on the daily Single National Price (“Prezzo Unico Nazionale” or “PUN”) calculated as an equally weighted average of all 24 hourly spot prices for that particular day. The contracts are quoted in €/MWh and traded on the European Energy Exchange (EEX), which represents Europe’s leading marketplace for energy and commodity products.

We considered contracts for seven different maturities: from 1 (labeled as Ec1) to 6 months (labeled as Ec6), representing the short to medium term contracts; 1 year to expiration (labeled as Ec12) was also included to represent the long-term contract. The total number of observations is 1655, covering the period from March 3, 2017 up to September 15, 2023. The time-span ensures a considerable amount of data containing different steady and spiky periods with futures curves exhibiting frequent temporary reversals. In this way we were able to verify and validate the effectiveness and robustness of the DRNNs under different market conditions.

Fig. 6 illustrates the dynamics of the price time series of the seven futures contracts together with the behavior of the corresponding log-returns.

All prices show a relatively stable trend until the beginning of 2021. However, between January 2021 and December 2022, it is possible to observe an unprecedented increase in the price level across all the given maturities mainly driven by the recent global COVID-19 pandemic and the new Russia-West confrontation [64] that caused acute global supply chain and energy shortage issues.

The latter becomes more evident when analyzing the dynamics of the log-returns series illustrated in Fig. 6. In fact, increasing volatility in futures returns across all maturities emerges throughout the mid-2021–end-2022 period, marked by significant positive and negative changes within a short time.

In general, the time series of daily futures log-returns exhibit significant changes in their volatility dynamics across the whole time span, as confirmed by the behavior of the moving variance determined for the log-returns series at each maturity and plotted in Fig. A.14 in Appendix A, thus suggesting the presence of heteroscedasticity; moreover, positive and negative spikes are also observed for all maturities as well as a decreasing volatility pattern for longer maturities.

Table 1 provides the descriptive statistics of the electricity futures prices dataset and their log-returns, including Mean, Standard Deviation (SD), Median, Minimum (Min), Maximum (Max), Skewness, Kurtosis and the results of the Jarque–Bera Test for normality, to give an insight into the nature of the underlying distribution.

The data confirm high volatility in each price series; moreover huge positive spikes can be observed for all maturities in the period of greater market turmoil, with record high peaks going over 700 €/MWh on average. By comparing the latter outcome with the average values calculated using the Min and Median columns of the price series in Table 1, it turns out that it is 23 times larger than the lowest price level and 12 times larger than the average median value.

Moving to the log-returns series and analyzing their distribution, the results show significant departures from Normality. The Ec1, Ec2, Ec3 series are characterized by positive skewness; on the contrary, Ec4, Ec5, Ec6, Ec12 exhibit a leptokurtic left-skewed distribution with greater probability of negative outlying returns.

In addition to the daily power futures prices, we collected the data on various assets with the aim of testing whether considering exogenous factors can lead to improvements in the model’s prediction performance. In this regard, prices for fossil fuels (natural gas and coal) and carbon emissions were taken into consideration after reviewing studies in the literature [16,76]. We included the historical gas and coal prices as they represent the main sources of fuel for fossil-fueled power plants in the European Union (EU) which, in turn, contribute to over the 39 % of electricity generation in the EU [59]. With regard to emission allowances, energy companies regulated by the European Emissions Trading System (EU-ETS) must acquire the certificates for every tonne of CO₂ they emit within one calendar year, hence fluctuations in CO₂ prices can lead to changes in the supply side structure and, consequently, in the price of the power market. Therefore, these variables represent important electricity generation costs which relevantly influence electricity futures prices dynamics.

In particular, we used the Dutch Title Transfer Facility (TTF) futures prices for Natural Gas, the API2 Rotterdam futures prices for Coal, as well as the EEX spot price series for Carbon Emission Certificates (CO₂) under the European Emissions Trading System. These variables were managed as time-dependent exogenous features and used together with the electricity futures prices as inputs to neural networks to get multivariate forecasts. The datasets of the exogenous variables were extracted from Thomson Reuters Datastream. In Appendix A, Fig. A.15 shows the temporal evolution of electricity prices at each maturity along with the related exogenous variables. To ensure uniformity with the data structure of electricity futures, for all the examined exogenous series we took daily values covering the same time horizon, from March 3, 2017 up to September 15, 2023. Moreover, for the NG and Coal futures contracts we selected the same maturities which we labeled by NGc1, NGc2, NGc3, NGc4, NGc5, NGc6, NGc12 and as Cc1, Cc2, Cc3, Cc4, Cc5, Cc6, Cc12 respectively; the CO₂ spot contract was indicated by Cc1.

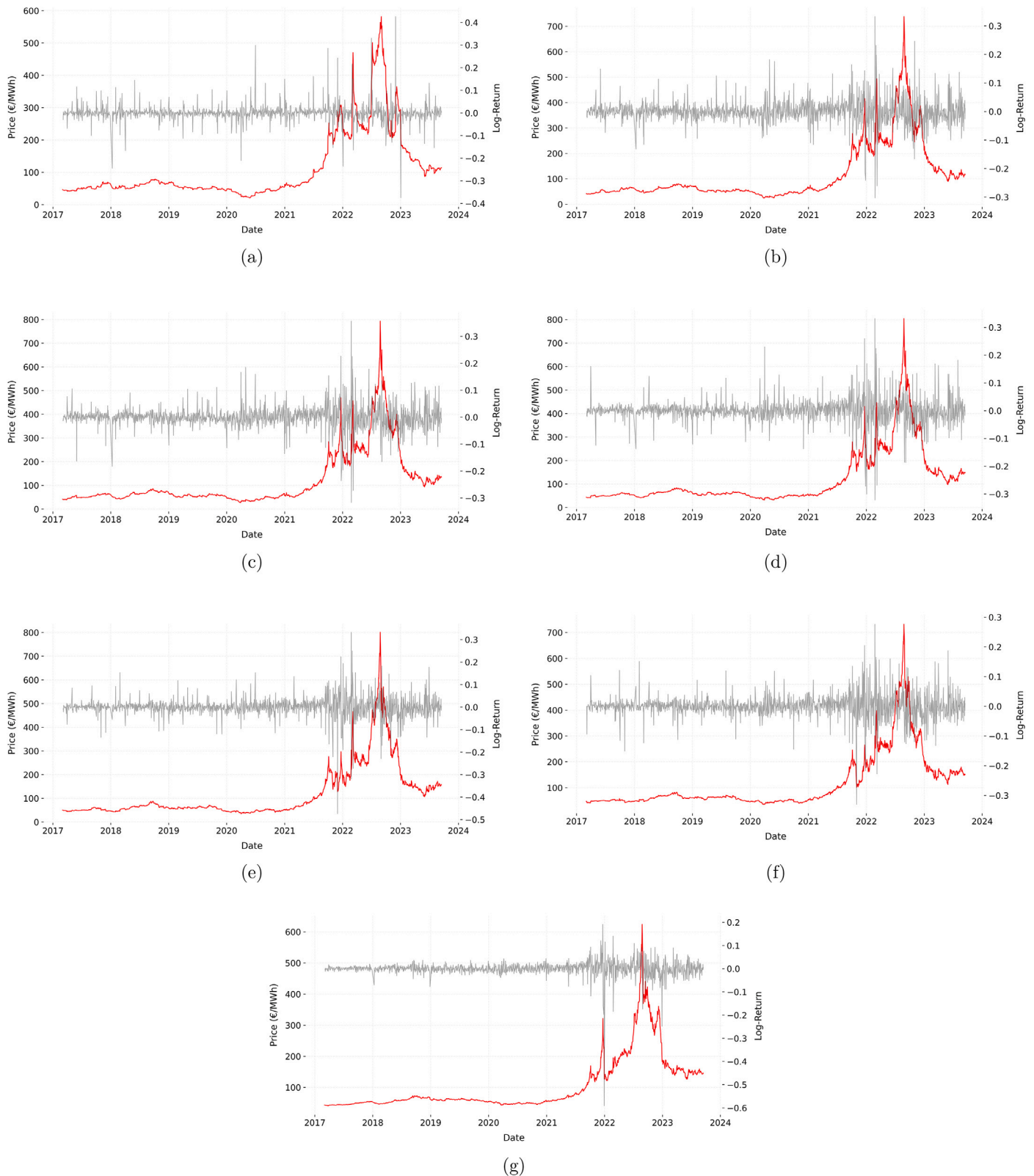


Fig. 6. Time series of daily closing prices (red) and log-returns (grey) on the Ec1 (a), Ec2 (b), Ec3 (c), Ec4 (d), Ec5 (e), Ec6 (f) and Ec12 (g) futures contracts. Time is represented on the x-axis, futures prices expressed in Euros are on the y-axis, while price log-returns are represented on the secondary y-axis (right hand side of the plot).

Since these variables represent important drivers of power prices, they are also expected to exhibit a significant degree of correlation with electricity futures prices, thereby embedding a relevant amount of useful

information about the movements of futures prices. To measure the strength of the relationship occurring between the considered datasets, we calculated the Spearman correlation coefficient (ρ) between each

Table 1

Descriptive statistics of futures prices (upper panel) and log-returns (lower panel) for each maturity. For the prices, we reported the Mean, the Standard Deviation (SD), the Median, the Minimum (Min), and the Maximum (Max) values, while for the log-returns we examined the Mean, the Standard Deviation, the Median, the Minimum, the Maximum, the Skewness, the Kurtosis and the results of the Jarque–Bera Test for normality (JB Test). The symbol * is used to denote the rejection of the null hypothesis H_0 (data are normally distributed) at the 1 % significance level.

	Maturity	Ec1	Ec2	Ec3	Ec4	Ec5	Ec6	Ec12
Prices	Mean	111.41	116.24	119.04	119.68	118.41	116.73	104.93
	SD	106.06	114.17	117.74	118.26	114.20	109.44	89.66
	Median	60.75	62.95	63.09	63.75	63.58	63.75	60.94
	Min	21.39	25.25	27.72	32.06	35.35	35.69	41.25
	Max	581.90	738.65	793.75	804.47	801.14	732.41	624.58
Log-returns	Mean	5.5×10^{-4}	6.3×10^{-4}	7.1×10^{-4}	7.4×10^{-4}	6.9×10^{-4}	7.1×10^{-4}	7.3×10^{-4}
	SD	3.6×10^{-2}	3.9×10^{-2}	3.9×10^{-2}	4.1×10^{-2}	4.1×10^{-2}	3.7×10^{-2}	2.9×10^{-2}
	Median	3.8×10^{-4}	5.9×10^{-4}	6.9×10^{-4}	7.1×10^{-4}	5.7×10^{-4}	6.4×10^{-4}	1.4×10^{-4}
	Min	-0.37	-0.30	-0.32	-0.32	-0.47	-0.33	-0.59
	Max	0.43	0.33	0.36	0.33	0.33	0.28	0.19
	Skewness	1.39	0.35	4.4×10^{-2}	-0.13	-0.99	-0.09	-5.76
	Kurtosis	38.91	14.20	16.29	17.01	24.48	13.68	114.43
	JB test	$8.9 \times 10^{4*}$	$8.7 \times 10^{3*}$	$1.2 \times 10^{4*}$	$1.3 \times 10^{4*}$	$3.2 \times 10^{4*}$	$7.8 \times 10^3*$	$8.6 \times 10^5*$

Table 2

Correlation between each electricity futures price series and the related price series of Natural Gas (second column), Coal (third column) and CO₂ (last column) contracts.

Maturity	ρ_{ElecNG}	$\rho_{ElecCoal}$	ρ_{ElecCO_2}
Ec1	0.41	0.31	0.13
Ec2	0.72	0.47	0.30
Ec3	0.73	0.47	0.33
Ec4	0.68	0.43	0.34
Ec5	0.69	0.44	0.30
Ec6	0.67	0.42	0.32
Ec12	0.74	0.47	0.42

electricity futures price series with the related counterparty in the NG, Coal and CO₂ datasets, and the results are provided in Table 2.

It can be seen that electricity futures are significantly affected by all the influencing factors; the strongest positive correlation is shared with the NG data, averaging just over 0.66. Conversely, the weakest positive correlation is shared with the CO₂ dataset: the lowest values are associated with shorter maturities, while they increase for longer ones, showing an average value of 0.31. Overall, the obtained results endorsed the use of the above described exogenous factors.

Notwithstanding the low ρ_{ElecCO_2} values at shorter maturities, all the three datasets were selected as input features in the forecasting models since these assets are known [42,92] to relevantly affect electricity futures price dynamics.

4. Empirical evaluation

4.1. Experiment setup

We explored the capabilities of the DRNN models introduced in Section 2 to make stable and robust predictions of electricity futures curves. The forecasting process was carried out following two alternative settings as described in Fig. 7 that shows the flowchart of the experimental design.

At first, we used the univariate electricity futures price prediction process (UEFPP). For this task the NAR-NN, the Univariate LSTM-NN (U-LSTM-NN), the Univariate Stacked LSTM-NN (U-ST-LSTM-NN), the Univariate Bidirectional LSTM-NN (U-BI-LSTM-NN) and the Univariate Encoder–Decoder LSTM-NN (U-ED-LSTM-NN) models were implemented to predict prices at each maturity based only on its past data readings, that is using only the information content of its own past values:

$$Ec_{i,t} = \theta(Ec_{i,t-1}, Ec_{i,t-2}, \dots, Ec_{i,t-k}), \quad i = 1, 2, 3, 4, 5, 6, 12 \quad (11)$$

where $Ec_{i,t}$ is the predicted price value at time t , while $Ec_{i,t-p}$ ($p = 1, \dots, k$) are the k past price values of the i -th maturity representing the networks input vector.

On the other hand, in the multivariate prediction process (MEFPP) we used the NARX-NN, Multivariate LSTM-NN (M-LSTM-NN), Multivariate Stacked LSTM-NN (M-ST-LSTM-NN), Multivariate Bidirectional LSTM-NN (M-BI-LSTM-NN) and Multivariate Encoder–Decoder LSTM-NN (M-ED-LSTM-NN) methods to predict prices of each maturity individually, based on historical data including the exogenous covariates described in Section 3:

$$Ec_{i,t} = \psi(Ec_{i,t-p}, NGc_{i,t-q}, Cc_{i,t-l}, COc_{1,t-m}), \quad i = 1, 2, 3, 4, 5, 6, 12 \quad (12)$$

where $Ec_{i,t}$ is as above, while $Ec_{i,t-p}$, $NGc_{i,t-q}$, $Cc_{i,t-l}$ and $COc_{1,t-m}$ (with $p, q, l, m = 1, \dots, k$) represent the k past values of the Electricity, Natural Gas and Coal futures prices time series at maturity i and CO₂ spot price series, respectively.

Moreover, given the unprecedented turmoil in energy markets observed during recent years, we divided the whole dataset into two subperiods and conducted both the UEFPP and MEFPP in two distinct time frames to validate the models' predictive power. The first subperiod was chosen as the more stable and less volatile one, while the second subperiod was characterized by price spikes and overall higher variance. The dataset in each subperiod was split into Training and Validation batches to set up the models on historical and unseen data, and into a Testing batch in order to assess their performance on future data.

In particular, the first subperiod ranges from March 3, 2017 to July 8, 2020 and is made up of 839 daily futures prices. Here observations from March 3, 2017 to March 25, 2019 were used as the training batch for model training and estimation. The period from March 26, 2019–September 13, 2019 corresponds to the validation set and was used to assess the model configuration on unseen data, while the interval ranging from September 16, 2019 to July 8, 2020 (labeled as Test Set 1) was employed for out-of-sample forecasting. The training, validation and test samples are made up of 515, 120 and 204 daily futures prices, respectively.

The second subperiod goes from March 3, 2017 to September 9, 2022 and contains 1395 daily futures prices; the data from March 3, 2017 to June 3, 2021 were set as the training sample, the data between June 4, 2021 and November 19, 2021 were used for validation, while the period ranging from November 22, 2021 to September 9, 2022 (labeled as Test Set 2) was employed for out-of-sample forecasting. Here the training, validation and test sets contain 1071, 120 and 204 days, respectively.

With regard to Test Set 1 and Test Set 2, Panel A and Panel B of Table 3 provide descriptive statistics of the two test batches, respectively, while Fig. 8 depicts the notched boxplot of electricity futures

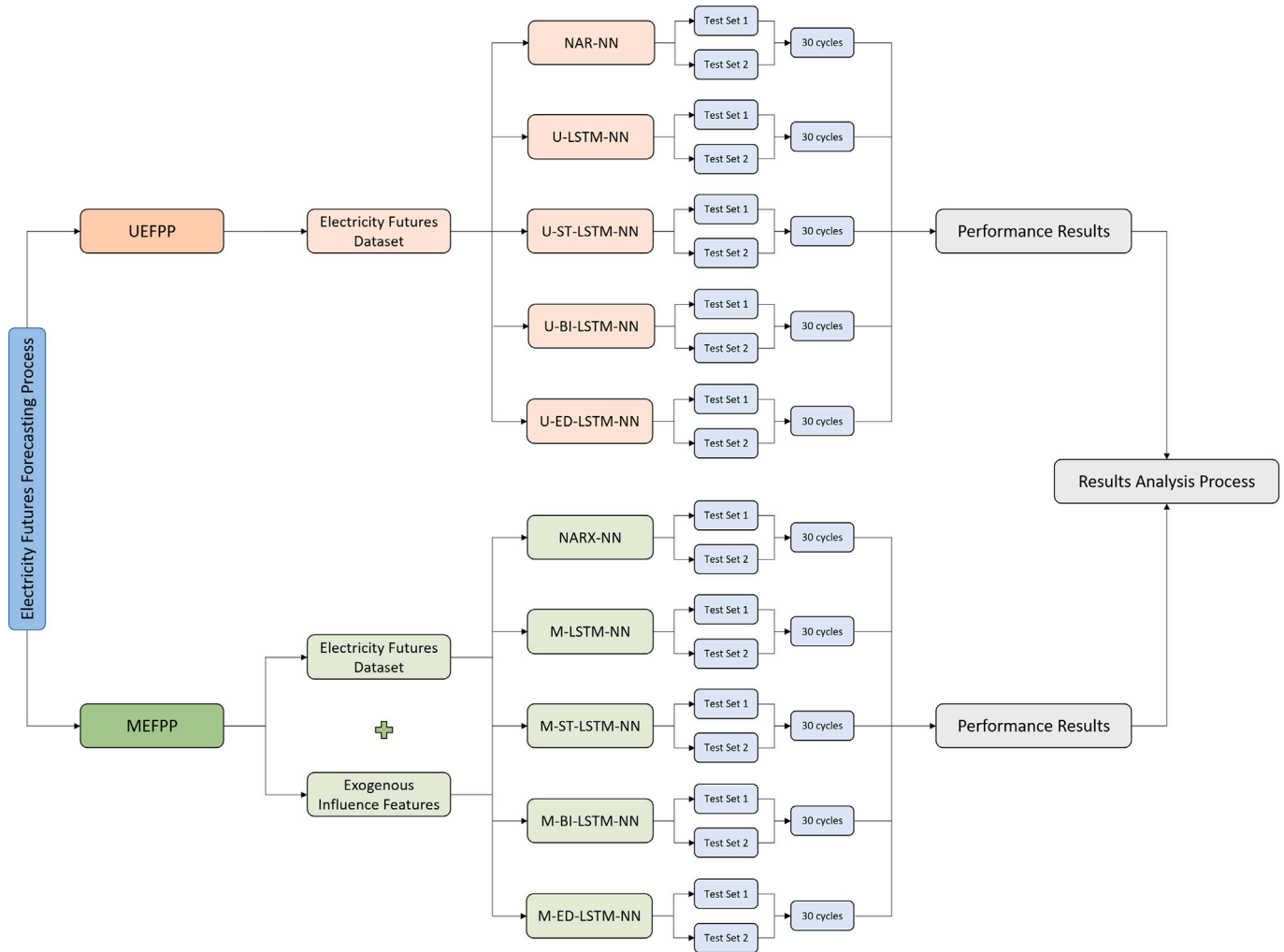


Fig. 7. Workflow of our forecasting framework. Prefixes U and M are abbreviations for Univariate and Multivariate, respectively.

prices at different maturities for the two test sets giving an insight into the distribution as well as the variability of the data over the various years of the time series.

By comparing the two sets it can be seen that price series differ significantly in terms of level, range, standard deviation and distribution. In fact, the level of prices and the standard deviation across the spectrum of maturities in Test Set 2 are at least 6 and 10 times higher compared to Test Set 1, respectively. Moreover, by visually analyzing Fig. 8 it can be noted that the length of the whiskers within Test Set 2 is significantly larger than in Test Set 1, thus suggesting that price series at each maturity exhibit higher dispersion of the data lying below the first quartile and above the third quartile. Furthermore, an analysis of both the price distribution and range of prices between the second and third quartiles within Test Set 2 suggests the presence of frequent and heavy price peaks. Additionally, Test Set 2 contains larger outliers exceeding only the upper whisker limit. Such extreme values are more than 1.5 times the interquartile range. This implies that the considered models are engaged in predicting price series with very spiky price behavior, thus representing the ideal background to stress test the neural networks, hence making the analysis more robust.

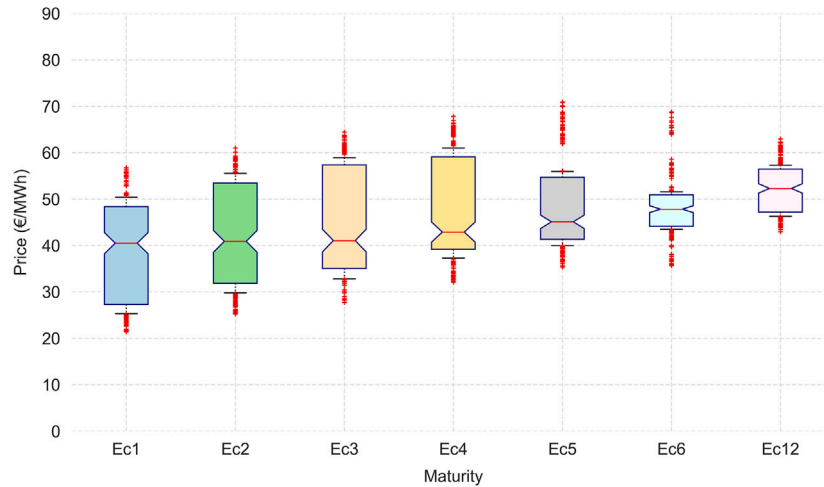
For either test set in both the UEFPP and MEFPP settings, each maturity’s price prediction was run on a daily basis using the sliding window method, for an overall number of 408 predicted days.

As pointed out in [66] there isn’t any rule of thumb for network topology and hyperparameter optimization. We therefore carried out a trial and error approach and examined various model settings considering different combinations of feedback delays, activation functions, number of nodes, cells, hidden layers and learning algorithms. Relatively to the NAR-NN and NARX-NN methods a good compromise was found by selecting one hidden layer, 5 delays, and 10 hidden neurons for NAR-NN and 15 for NARX-NN; additionally, for both models the sigmoid (linear) activation function was used for the hidden (output) neurons while the Levenberg–Marquardt Backpropagation learning rule was chosen for network training and learning. With regard to the LSTM-based neural networks in both the univariate and multivariate settings, the best solution turned out to consist of 1 layer with 200 units for the LSTM-NN and BI-LSTM-NN, 3 layers with 200 units for the ST-LSTM-NN, and 1 layer with 100 units in both the encoder and decoder; all models were trained in a supervised learning fashion for 1000 epochs using the Adaptive Moment Estimation (ADAM) optimization algorithm [67]. The code for the implementation of the proposed methodology and models was developed in MATLAB R2024a for the NAR-NN and NARX-NN methods, and in Python (3.11.7) using the open-source Keras (2.13.1) library [26] with TensorFlow (2.13.1) as backend for the LSTM-based neural network models.

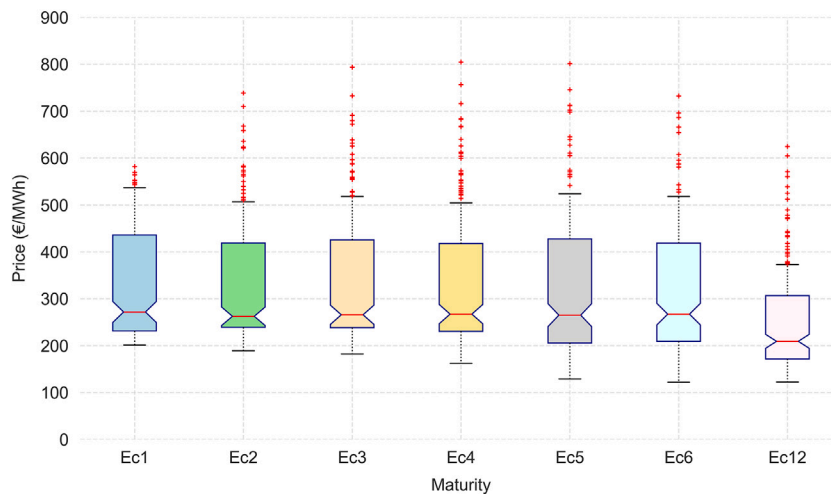
Additionally, given the stochastic nature of ANN models, we run thirty repeated forecast cycles using averaged forecasted results as the

Table 3
Descriptive statistics of electricity futures prices for Test Set 1 (Panel A) and Test Set 2 (Panel B).

	Maturity	Ec1	Ec2	Ec3	Ec4	Ec5	Ec6	Ec12
Panel A. Test Set 1	Mean	38.98	41.93	44.49	46.51	47.54	47.92	51.81
	SD	10.85	10.92	10.83	10.46	8.59	5.92	4.99
	Min	21.39	25.25	27.72	32.06	35.35	35.69	42.96
	Max	56.75	61.00	63.53	66.35	68.55	65.82	62.12
Panel B. Test Set 2	Mean	317.78	329.09	330.20	326.84	317.66	312.33	243.68
	SD	109.94	126.26	132.64	142.28	143.76	134.68	106.15
	Min	201.49	189.07	182.00	162.37	128.94	121.92	122.20
	Max	581.90	738.65	793.75	804.47	801.14	732.41	624.58



(a)



(b)

Fig. 8. Notched boxplot of electricity futures prices at different maturities for Test Set 1 (a) and Test Set 2 (b). The orange line inside the boxes indicates the median value; the “notch” denotes the 95 % Confidence Interval of the median; the box represents the Interquartile Range (IQR) containing the 50 % of the observations, while the lower and upper whiskers represent the 25 % of the data each, excluding the outliers; finally, the red points identify the outliers.

final model’s outcome. This is to ensure robust results and to reduce the randomness of the forecasts.

4.2. Baseline models

The forecasting framework discussed in the previous section was benchmarked against a set of established baseline methods with the aim

of facilitating a comprehensive assessment of the DRNN models’ efficacy and ensuring a robust evaluation framework.

The models were chosen to cover a range of both classical statistical methods and Machine Learning approaches commonly used in the EPF literature. All models were implemented in both univariate and multivariate settings. The main principles of each baseline model are briefly

outlined below. Readers can refer to the original papers for detailed descriptions and full documentation.

In particular, within the class of conventional statistical approaches we selected:

1. the Seasonal Autoregressive Integrated Moving Average (SARIMA) model [19], a forecaster that integrates autoregression, differencing, moving average components, along with seasonal components;
2. the Seasonal Autoregressive Integrated Moving Average with Exogenous Regressors (SARIMAX) model [94], a SARIMA model that incorporates exogenous predictors;
3. the Autoregressive model with Exogenous Regressors (ARX) [79], a simple linear autoregressive model, relates the current value of a target variable to its past values and the current and past values of exogenous variables.

The class of Machine Learning methods includes:

1. the Multilayer Perceptron (MLP) neural network [114], a standard NN that uses stacked layers of interconnected processing units to perform nonlinear mapping between input and output data, enables the network to capture and represent complex data features;
2. the Support Vector Regression (SVR) model [36], a forecaster that maps the input data into high dimensional feature space where linear functions are used to formulate nonlinear relationships between input and output.

Since we used advanced NN architectures capable of learning complex features and capturing temporal correlations in sequential/time series data, we chose the above benchmark models in order to replicate/achieve similar tasks. Specifically, on the one hand, we selected ARIMA-based models for their effectiveness in capturing time series dependencies, seasonal patterns as well as relationships with external factors, while on the other MLP and SVR serve as simpler machine learning baselines providing effective non-linear mapping capabilities.

Additionally, these models demonstrated relevant degrees of prediction accuracy within the EPF literature [16,127], while also being relatively simple to implement, interpretable, and computationally efficient.

To build the statistical models the Econometric Modeler App was used in conjunction with *ad-hoc* developed code within the MATLAB R2024a environment. For what it is concerning the Machine Learning models, the framework was developed in Python (3.11.7) making use of the Scikit-learn (1.5.1) [103] and Keras (2.13.1) libraries.

4.3. Results discussion

For a comprehensive evaluation of the predictive accuracy of the proposed models, this paper employs two widely used performance indicators, namely the Root Mean Squared Forecasting Error (RMSFE):

$$\text{RMSFE} = \sqrt{\frac{1}{n} \sum_{t=1}^n (x_{t+h}^{\text{obs}} - x_{t+h})^2}, \quad (13)$$

which measures the standard deviation of prediction errors, and the Mean Absolute Percentage Error (MAPE):

$$\text{MAPE} = \frac{100}{n} \sum_{t=1}^n \left| \frac{x_{t+h}^{\text{obs}} - x_{t+h}}{x_{t+h}^{\text{obs}}} \right|, \quad (14)$$

which returns the mean of the absolute percentage errors of predictions. In both 13 and 14, x_{t+h}^{obs} and x_{t+h} represent the observed and predicted values respectively, n denotes the sample size while h is the forecast horizon.

The out-of-sample forecasting results are firstly presented in Table 4, highlighting in bold the best performing method outcome. For each test set and model we summarized the Mean, the Standard Deviation (SD), the Minimum (Min) and the Maximum (Max) of the RMSFE and MAPE accuracy metrics.

An analysis of the DRNNs results indicates that all the implemented techniques exhibit a highly satisfactory performance, ensuring an average MAPE score greater than 97 % within Test Set 1 and greater than 91 % within Test Set 2, thereby acting as good predictive techniques.

Considering Test Set 1, it is possible to conclude that the M-BI-LSTM-NN and M-ST-LSTM-NN models significantly outperform the other competing methods reporting the best RMSFE and MAPE scores (almost at par), followed by the NAR-NN and M-LSTM-NN models, which exhibit quite close results. More specifically, considering, for instance, the MAPE metric the M-BI-LSTM-NN, M-ST-LSTM-NN, NAR-NN, and M-LSTM-NN models achieved 98.11 %, 98.10 %, 98.04 %, and 98.01 % predictive accuracies, respectively. All the other methods reported lower scores, around 97.5 % on average; here the U-ST-LSTM-NN, M-ED-LSTM-NN and the NARX-NN models reported the lowest accuracy measures of 97.86 %, 97.86 % and 97.62 %, respectively.

It can be noted that incorporating exogenous factors provides a relevant boost only to three models out of five, i.e. to the LSTM-NN, ST-LSTM-NN and BI-LSTM-NN performance. In fact, the M-LSTM-NN, the M-ST-LSTM-NN and the M-BI-LSTM-NN reduced the MAPE (RMSFE) score by 6.13 % (7 %), 11.22 % (8 %) and 5.97 % (2 %), respectively.

With regard to Test Set 2, the U-ED-LSTM-NN model ensured the best performance in the day-ahead predictions, with 95.33 % precision; furthermore, the model showed an almost halved RMSFE score with respect to the NAR-NN and NARX-NN models. Such result is due to the U-ED-LSTM-NN model's enhanced memory abilities which allow it to capture and store nonlinear patterns embedded in past futures price data. The second place is taken by the U-ST-LSTM-NN model with 95.21 % accuracy; in the third place, we find the U-BI-LSTM-NN model with 95.16 % accuracy, followed by the U-LSTM-NN model with 95.10 % accuracy. The multivariate LSTM based models achieved accuracy scores ranging between 94.32 % and 94.81 %. Relatively to the M-BI-LSTM-NN model, which was the best in Test Set 1, it generated a poorer performance: the predictive precision decreased from 98.11 % (Test Set 1) to 94.81 % (Test Set 2), while the RMSFE increased by 22 times compared to the score achieved in Test Set 1. A similar deterioration of the metrics is also observed for the other LSTM-based models, and even worse in the case of the NAR-NN and NARX-NN models whose RMSFE (MAPE) scores increased by at least 33 (4) times.

With respect to Test Set 2, it is noteworthy that adding exogenous features does not bring improvements to the model families, rather it appears to weaken their accuracy. However, this fact is in contrast with the results observed in Test Set 1. In our opinion, such a difference is mainly related to the trends of the examined series. In fact, all series within Test Set 1 show very close and similar dynamics (without jumps or drops), therefore exogenous features carry useful information capable of increasing the models' predictive accuracy. On the contrary, Test Set 2 is characterized by both a spiky behavior of electricity futures price series and at the same time less volatile price dynamics of exogenous features which, as a consequence, do not hold any useful latent information content and thus do not bring any positive contribution to the models' predictive power.

The performance comparison of the univariate and multivariate DRNN models is also shown in Figs. 9–12 where we illustrate for each maturity in the test sets, the models day-ahead forecasting results, and in Fig. 13 where we display for each test set the average actual and predicted futures curves. Based on the visual analysis of the graphs, the following conclusions can be drawn: (i) all the models forecast trends are close enough to the observed trends and do not exhibit unreasonable spikes or drops; (ii) considering the price time series, NAR-NN and NARX-NN models tend to exhibit a more erratic behavior with respect to other methods; (iii) when peak values occur, the

univariate and multivariate LSTM based models show a smoother overall behavior.

Finally, it is noteworthy to highlight that the LSTM-based models maintain good performance even in extreme conditions, such as those characterizing Test Set 2, without being particularly affected by turmoil. In fact, in the face of a significant increase in the price level across the whole maturity spectrum by at least 6 times with respect to Test Set 1, the reduction in predictive accuracy is maintained in the range of 2.67 % – 3.85 %, which remains above 91 %. However, the Multivariate Bidirectional LSTM-NN model that performed better in the first test set was unable to maintain its higher predictive power during the most unstable period.

By comparing the forecasting results of the neural network and baseline models summarized in Table 4, it turns out that almost all the univariate DRNN models, along with the overwhelming majority of the multivariate ones, outperform their respective univariate/multivariate competitors.

Considering Test Set 1, the DRNNs achieved 98 % predictive accuracy on average, while the baseline competitors showed lower scores, around 96 % on average. Within Test Set 2, the neural networks ensured, on average, 94 % precision, while their competitors reported a lower accuracy measure, that is 93 % on average.

For what it concerns the best performing methods, the SARIMA performs relatively well among the baseline models, achieving the best results within that group. Nevertheless, the M-BI-LSTM-NN and the U-ED-LSTM-NN stand out by showing the lowest MAPE metric. Overall this demonstrates greater DRNNs’ flexibility and adaptability

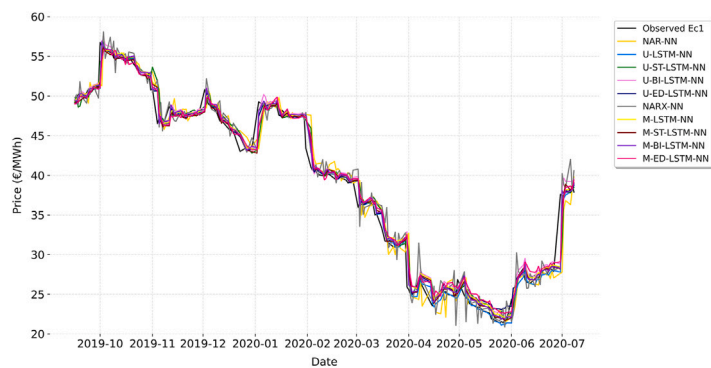
to a wide variety of dynamics and trends characterizing the electricity futures term structure, resulting in higher accuracy, lower variability and very small magnitudes of the error metrics, hence underscoring the superior efficacy of the ML approach. Such success can be attributed to the networks’ ability to perform nonlinear mapping, as well as their use of backward and forward temporal links and dynamic memory. The predictive performance clearly demonstrated the consistency of the implemented forecasting strategy. In this way, our results highlight that the ML-based approach is the preferable strategy for day-ahead electricity futures curve forecasting providing the lowest errors.

To statistically validate the superior predictive power of the M-BI-LSTM-NN within Test Set 1 and of the U-ED-LSTM-NN within Test Set 2 over all other competing models, we moved one step further and performed the one-sided Harvey–Leybourne–Newbold (HLN) Test [50]. This test verifies the statistical significance of outperformance of a selected method compared to other methods. In our case study we set the models with the lowest MAPE, i.e. the M-BI-LSTM-NN and the U-ED-LSTM-NN, as the benchmark in their respective test sets and then compared each of the other sets of forecasts to the benchmark forecast to determine whether the benchmark models provide significantly more accurate predictions. In particular, the HLN Test statistic tests the null hypothesis H_0 that predictions of the benchmark model (Method 1) are more accurate than those of the competing model (Method 2), against the alternative H_1 that predictions of the benchmark model (Method 1) are less accurate than those of the competing one (Method 2), at 95 % significance level.

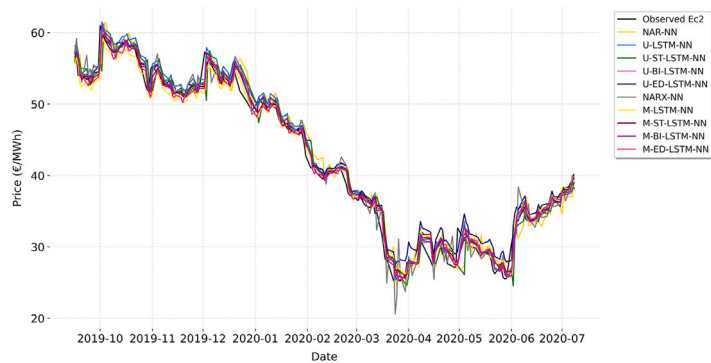
Table 4

Average MSFE and MAPE (%) metrics obtained with different competing methods. In every Test Set, the DRNN and BM panels relate to the Dynamic Recurrent Neural Network and Baseline Models, respectively. Models with the best performance are highlighted in bold.

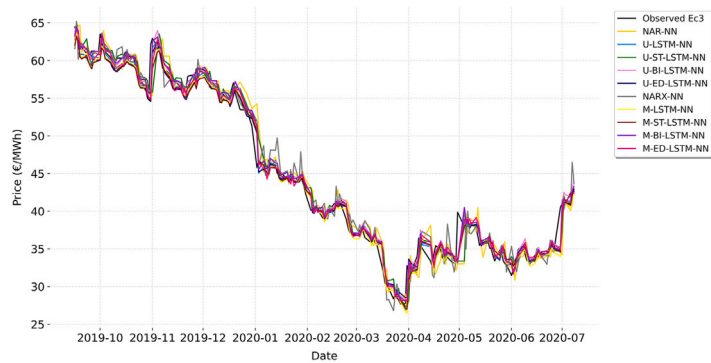
				RMSFE				MAPE (%)			
		Method	Mean	SD	Min	Max	Mean	SD	Min	Max	
Test Set 1	DRNN	NAR-NN	1.24	0.23	0.74	1.41	1.96	0.47	1.08	2.55	
		U-LSTM-NN	1.31	0.27	0.89	1.81	2.12	0.84	1.44	3.98	
		U-ST-LSTM-NN	1.30	0.29	0.75	1.71	2.14	0.70	1.20	3.47	
		U-BI-LSTM-NN	1.24	0.28	0.71	1.67	2.01	0.75	1.13	3.53	
		U-ED-LSTM-NN	1.27	0.31	0.68	1.69	2.05	0.64	1.03	3.10	
		NARX-NN	1.43	0.31	0.74	1.67	2.38	0.62	1.16	3.00	
		M-LSTM-NN	1.22	0.23	0.70	1.37	1.99	0.49	1.06	2.49	
		M-ST-LSTM-NN	1.20	0.19	0.79	1.35	1.90	0.39	1.20	2.48	
		M-BI-LSTM-NN	1.22	0.22	0.73	1.39	1.89	0.35	1.12	2.10	
		M-ED-LSTM-NN	1.29	0.19	0.87	1.50	2.14	0.40	1.30	2.58	
	BM	SARIMA	1.20	0.26	0.66	1.40	1.93	0.53	1.01	2.65	
		U-MLP	1.38	0.21	0.99	1.70	2.29	0.44	1.58	2.81	
		U-SVR	1.33	0.37	0.69	1.86	2.40	1.13	1.07	4.40	
		ARX	1.46	0.40	0.72	1.82	2.30	0.70	1.12	3.38	
		SARIMAX	2.73	1.04	1.57	4.06	4.53	1.92	2.32	6.63	
		M-MLP	1.92	0.78	1.24	3.54	3.58	1.75	1.94	6.99	
	M-SVR	2.18	0.59	1.55	3.17	4.60	1.87	2.63	7.49		
Test Set 2	DRNN	NAR-NN	48.12	16.20	20.12	66.74	8.01	2.19	3.50	10.09	
		U-LSTM-NN	23.79	4.63	17.19	28.09	4.90	0.87	3.59	5.65	
		U-ST-LSTM-NN	23.66	4.91	16.49	29.44	4.79	1.10	2.80	5.82	
		U-BI-LSTM-NN	23.52	4.27	17.76	27.96	4.84	0.90	3.39	5.69	
		U-ED-LSTM-NN	23.46	5.43	16.50	30.03	4.67	1.04	2.74	5.94	
		NARX-NN	46.70	10.60	30.35	57.75	8.85	1.53	5.60	10.35	
		M-LSTM-NN	26.95	6.11	17.85	37.07	5.40	1.17	3.30	6.84	
		M-ST-LSTM-NN	27.29	6.48	19.70	37.06	5.68	1.58	3.41	8.40	
		M-BI-LSTM-NN	26.23	4.23	19.98	30.68	5.19	0.96	3.58	6.37	
		M-ED-LSTM-NN	25.66	3.70	19.99	30.34	5.48	1.28	3.39	7.52	
	BM	SARIMA	23.19	5.67	15.99	28.95	4.92	1.14	2.78	6.13	
		U-MLP	25.07	5.15	17.50	30.91	5.35	1.07	3.41	6.37	
		U-SVR	39.53	5.84	30.12	45.07	7.68	1.30	4.93	8.83	
		ARX	26.41	4.04	19.97	31.70	5.22	0.74	4.00	6.19	
		SARIMAX	38.78	15.02	24.02	60.67	7.83	3.27	4.03	13.23	
		M-MLP	29.44	9.87	18.81	44.06	5.99	2.31	3.81	10.53	
	M-SVR	49.34	5.29	39.49	54.17	9.02	0.86	7.27	10.02		



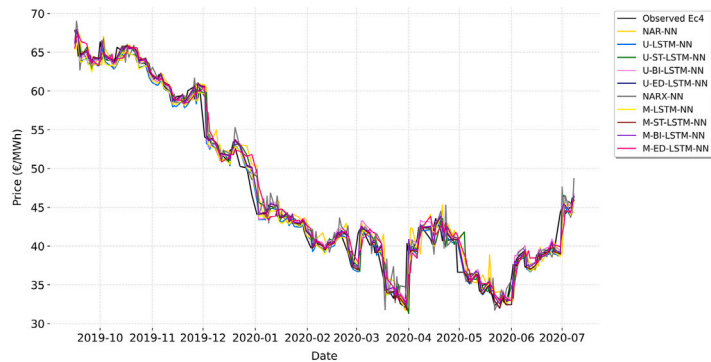
(a)



(b)

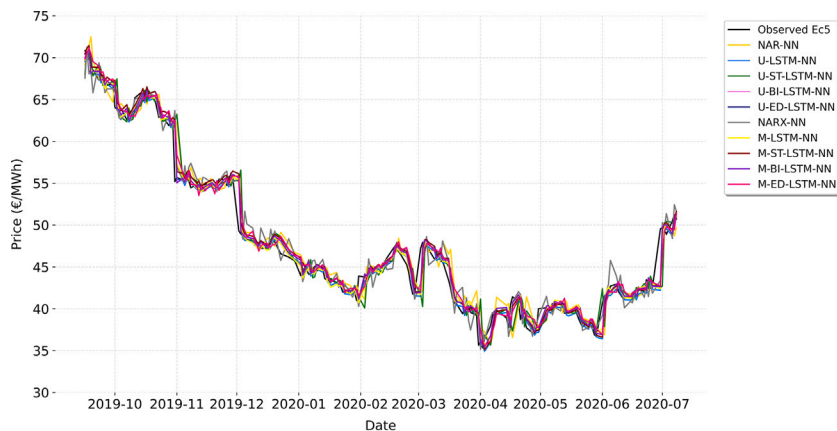


(c)

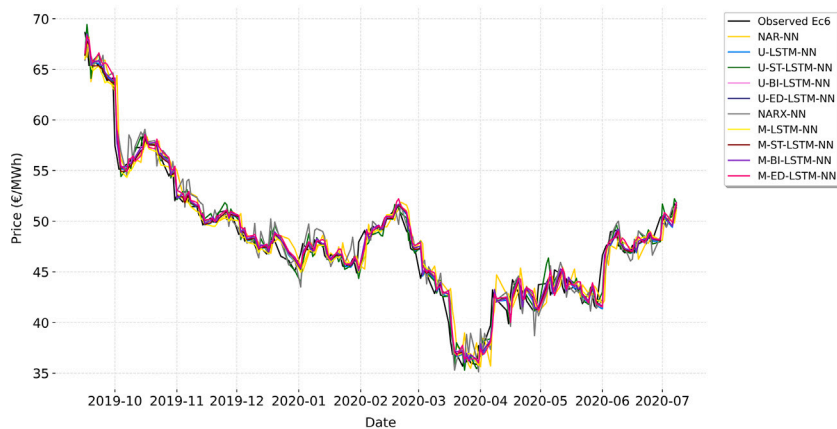


(d)

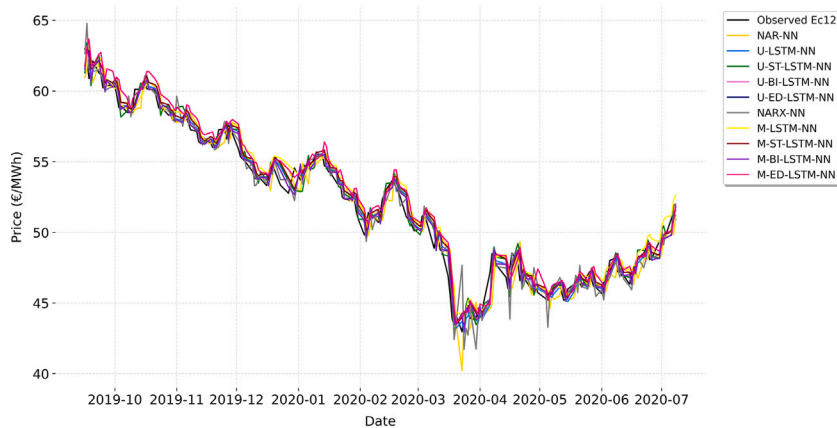
Fig. 9. Models point forecasts of the price series of the Ec1 (a), Ec2 (b), Ec3 (c), Ec4 (d) futures contracts within Test Set 1.



(a)

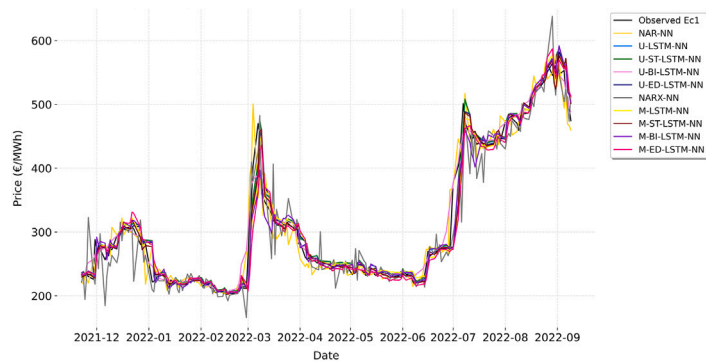


(b)

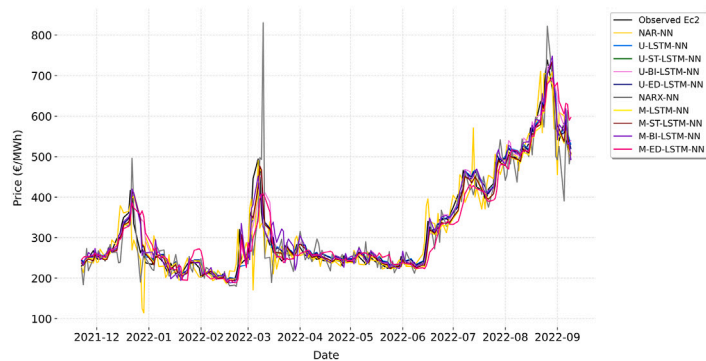


(c)

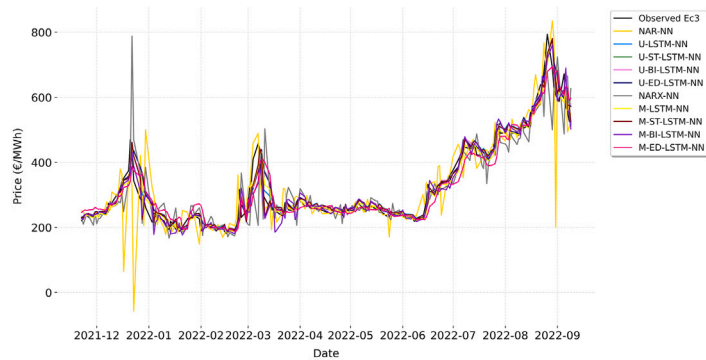
Fig. 10. Models point forecasts of the price series of the Ec5 (a), Ec6 (b) and Ec12 (c) futures contracts within Test Set 1.



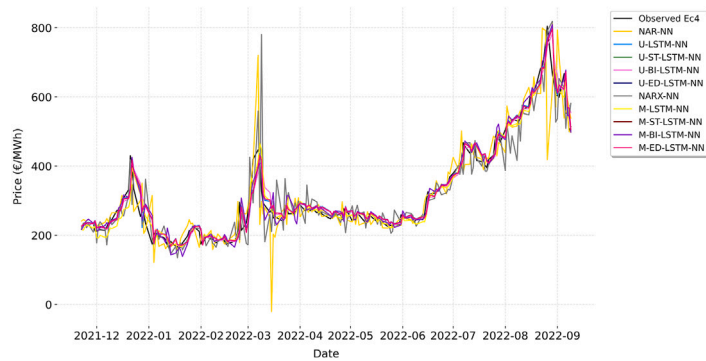
(a)



(b)

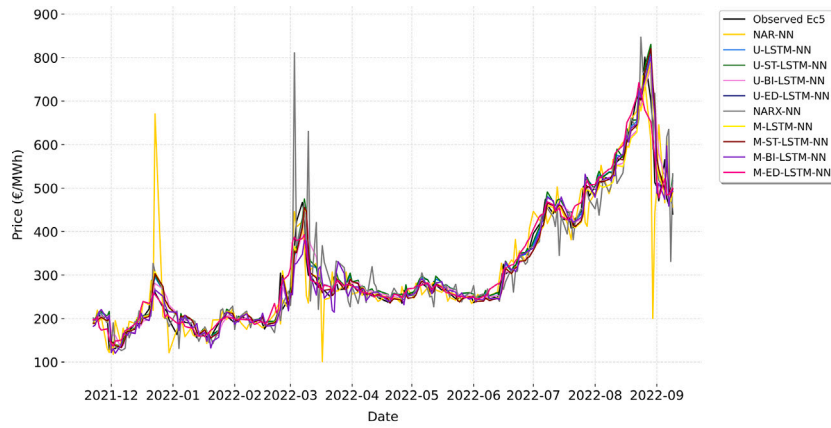


(c)

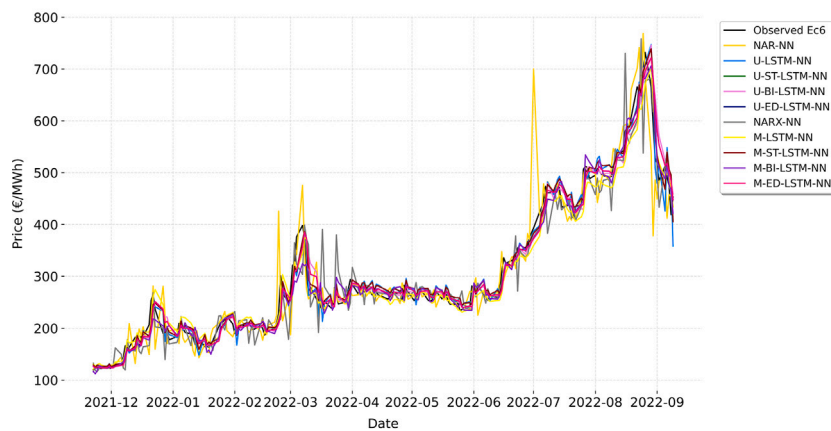


(d)

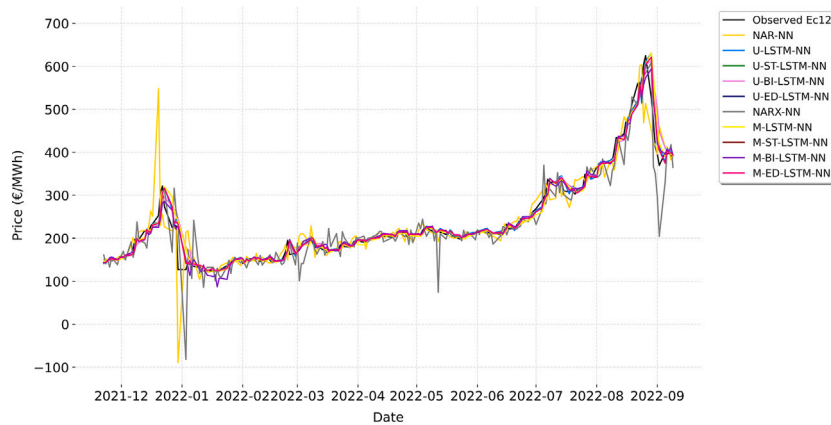
Fig. 11. Models point forecasts of the price series of the Ec1 (a), Ec2 (b), Ec3 (c), Ec4 (d) futures contracts within Test Set 2.



(a)



(b)



(c)

Fig. 12. Models point forecasts of the price series of the Ec5 (a), Ec6 (b) and Ec12 (c) futures contracts within Test Set 2.

The HLN test statistic used for the model’s prediction comparison follows a Student’s t -distribution with $(n-1)$ degrees of freedom and is described by:

$$HLN = \frac{\bar{m}}{\sqrt{\frac{2\pi \hat{f}_m(0)}{n}}} \sqrt{\frac{n+1-2h+h(h-1)}{n}} \sim t_{n-1} \quad (15)$$

where \bar{m} denotes the sample mean of the loss differential between two forecasts, $\hat{f}_m(0)$ is the consistent estimate of the zero-frequency spectral density of the loss differential, n is the sample size while h represents the forecast horizon ($h = 1$ in our case). Test results are reported in Table 5.

The scores (p -values) of the HLN Statistic reported in column three (four) of Table 5 are notably lower (higher) than the critical value at

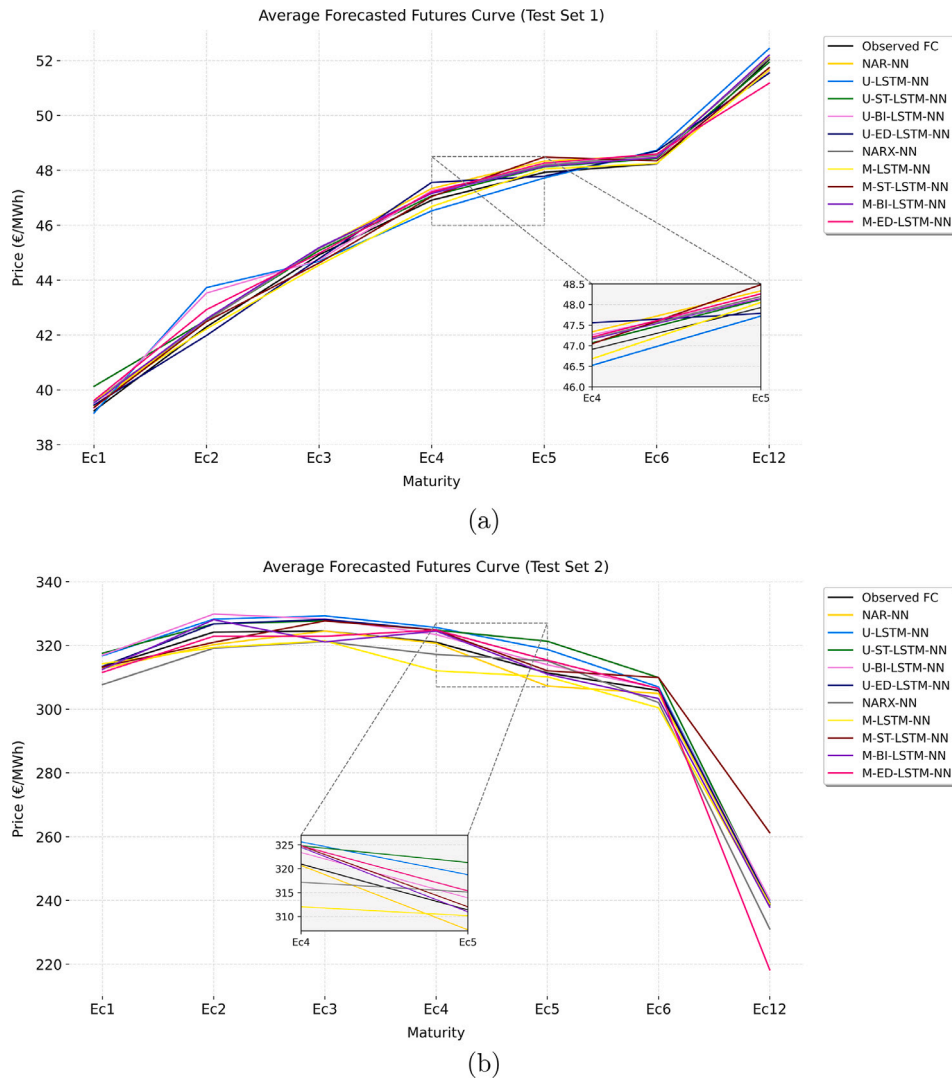


Fig. 13. Comparison of the Test Set 1 (a) and Test Set 2 (b) average observed futures curves with the average forecasted ones with different neural network models. The inset shows a zoomed-in area to highlight the predictive performance of the competing models.

95 % significance level $t_{0.05, n-1} = 1.645$ (0.05). This, in turn, implies that in all the examined comparisons, we've fallen within the acceptance region, thus strongly accepting the null hypothesis, i.e. predictions of the model indicated in the Column 1 are more accurate than those of the model indicated in Column 2. We can therefore conclude that the HLN test results are in line with those of the MAPE in Table 4 thus suggesting that the M-BI-LSTM-NN and the U-ED-LSTM-NN are the most accurate forecasting models within their test sets.

Overall, we can conclude that the proposed framework can (I) achieve satisfactory and consistent predictive results in both calm as well as volatile market conditions and (II) outperform well-established competitors in terms of both accuracy and forecast bias, thus confirming the adequacy and usefulness of the implemented deep learning models for predicting electricity futures curves.

5. Conclusion

In this study, we provided a univariate and multivariate deep learning framework to predict the term structure of electricity futures prices using Dynamic Recurrent Neural Networks (DRNNs). Our approach used the NAR-NN, NARX-NN, Univariate/Multivariate LSTM-NN, Univariate/Multivariate Stacked LSTM-NN, Univariate/Multivariate

Bidirectional LSTM-NN and Univariate/Multivariate Encoder-Decoder LSTM-NN models to capture the nonlinear temporal relationship of the data as well as complex hidden correlation features with various exogenous factors. The feasibility of the approach was investigated using two different time spans, that is a stable period (labeled as Test Set 1) and a period of global instability characterized by higher volatility and price peaks (labeled as Test Set 2) which were used as test sets to analyze and compare the models point forecast accuracy. Furthermore, a comparative study with popular statistical and ML methods was carried out to fully assess the robustness and effectiveness of the framework.

Experimental results showed that the proposed DRNN methods can effectively manage trends and dynamics characterizing electricity futures curves and thus provide their effective day-ahead predictions with an average predictive accuracy of over 94 %. The comparative analysis indicates that the NAR-NN and NARX-NN models reported good performance when used only in periods of relatively steady price dynamics. However, their simpler neural architectures do not provide sufficient flexibility to manage and predict price series characterized by huge spikes and drops, such as those observed within Test Set 2. On the other hand, the univariate and multivariate LSTM-based models exhibited good performance in Test Set 1 and, more importantly, superior

Table 5

Results of the Harvey–Leybourne–Newbold Test. The first column is Method 1, which is the benchmark model, while column two is Method 2, which is the competing model. In every Test Set, Panel A includes the comparison between the benchmark model and the competing DRNNs, while Panel B relates to the comparison between the benchmark model and the competing baseline models. The symbol * indicates acceptance of the null hypothesis H_0 (forecasts of Method 1 are more accurate than forecasts of Method 2) at 95 % significance level.

		Competing models	HLN statistic	p-value	
Test Set 1	Panel A	M-BI-LSTM-NN vs NAR-NN	-0.3461	0.6352*	
		M-BI-LSTM-NN vs U-LSTM-NN	-2.1967	0.9854*	
		M-BI-LSTM-NN vs U-ST-LSTM-NN	-0.2184	0.5863*	
		M-BI-LSTM-NN vs U-BI-LSTM-NN	0.2989	0.3826*	
		M-BI-LSTM-NN vs U-ED-LSTM-NN	0.0258	0.4897*	
		M-BI-LSTM-NN vs NARX-NN	-1.3832	0.9159*	
		M-BI-LSTM-NN vs M-LSTM-NN	-0.2745	0.6080*	
		M-BI-LSTM-NN vs M-ST-LSTM-NN	1.1493	0.1259*	
			M-BI-LSTM-NN vs M-ED-LSTM-NN	-0.6730	0.7491*
	Panel B	M-BI-LSTM-NN vs SARIMA	0.0482	0.4810*	
		M-BI-LSTM-NN vs U-MLP	-4.2200	0.9999*	
		M-BI-LSTM-NN vs U-SVR	-2.0140	0.9780*	
		M-BI-LSTM-NN vs ARX	-3.0780	0.9999*	
		M-BI-LSTM-NN vs SARIMAX	-2.9370	0.9980*	
		M-BI-LSTM-NN vs M-MLP	-4.9180	0.9999*	
		M-BI-LSTM-NN vs M-SVR	-5.8460	0.9999*	
Test Set 2	Panel A	U-ED-LSTM-NN vs NAR-NN	-3.0102	0.9985*	
		U-ED-LSTM-NN vs U-LSTM-NN	-1.4547	0.9263*	
		U-ED-LSTM-NN vs U-ST-LSTM-NN	0.0172	0.4931*	
		U-ED-LSTM-NN vs U-BI-LSTM-NN	-1.3469	0.9102*	
		U-ED-LSTM-NN vs NARX-NN	-4.1470	0.9999*	
		U-ED-LSTM-NN vs M-LSTM-NN	-1.4415	0.9245*	
		U-ED-LSTM-NN vs M-ST-LSTM-NN	-4.3338	0.9999*	
		U-ED-LSTM-NN vs M-BI-LSTM-NN	-1.2616	0.8957*	
			U-ED-LSTM-NN vs M-ED-LSTM-NN	-0.7497	0.7728*
	Panel B	U-ED-LSTM-NN vs SARIMA	0.1528	0.4390*	
		U-ED-LSTM-NN vs U-MLP	-1.8770	0.9700*	
		U-ED-LSTM-NN vs U-SVR	-6.8120	0.9999*	
		U-ED-LSTM-NN vs ARX	-2.4230	0.9920*	
		U-ED-LSTM-NN vs SARIMAX	-13.4900	0.9999*	
		U-ED-LSTM-NN vs M-MLP	-12.6600	0.9999*	
		U-ED-LSTM-NN vs M-SVR	-7.3680	0.9999*	

and stable results with respect to NAR-NN and NARX-NN within the more turbulent Test Set 2. In particular the analysis revealed that the M-BI-LSTM-NN model performed best within the calmer period, while the U-ED-LSTM-NN turned out to be the most effective approach within the most turbulent period.

Furthermore, we point out that although the basic LSTM-NN architecture represents an effective choice for electricity futures curve predictions, empirical evidence shows that its extensions in terms of improved architectures, that is Stacked-LSTM-NN, Bidirectional-LSTM-NN and Encoder–Decoder-LSTM-NN models, provide a significant boost in increasing the predictive performance mainly due to the enhanced memory abilities. Additionally, it’s worth noting that the use of exogenous input features does not always represent an added value in the forecasting process and their use is strongly dependent on the economic and geopolitical context, as testified by the results obtained within the two different time spans.

To conclude, empirical evidence demonstrated that the classical statistical and ML baseline models were outperformed by the overwhelming majority of the DRNN models in both univariate/multivariate settings. The LSTM-based neural network models showcased superior results due to their architecture and dynamic memory mechanism that enables them to manage complex nonlinear problems involving temporal dependencies as well as the chaotic features of power futures prices. Within this class the M-BI-LSTM-NN and the U-ED-LSTM-NN showed to achieve a predictive accuracy that is statistically significantly better not only compared to other neural network models, but also relative to all other baseline methods.

Nevertheless, despite the good results that have been obtained up to now, one of the main drawbacks of the modeling framework is the significant computational time. In this regard, future studies will explore alternative learning, validation and optimization techniques to reduce the computational time. We also acknowledge that our forecasting framework considered only a one-day-ahead time horizon. Thus, assessing the DRNNs performance for longer time horizons (e.g. three/five days, one/two weeks) may provide useful information to market players and regulators. Overall, there exists room for improvement. Future research may include the testing of alternative model configurations and combinations (e.g. Convolutional, Generalized Regression or Graph Neural Networks) as well as the insertion of attention mechanisms in the network’s architecture in order to consider the different contributions of historical data at different time steps. Additionally, the analysis of the effects on the model’s predictive power of different combinations of explanatory variables as well as examining the impact of different exogenous variables (e.g. big data, fundamental, financial, weather or geopolitical factors) can be beneficial. Actually all these topics represent a part of our ongoing research.

CRedit Authorship Contribution Statement

Oleksandr Castello: Writing – review & editing, Writing – original draft, Validation, Software, Methodology, Formal analysis, Data curation, Conceptualization. **Marina Resta:** Writing – review & editing, Validation, Supervision, Conceptualization.

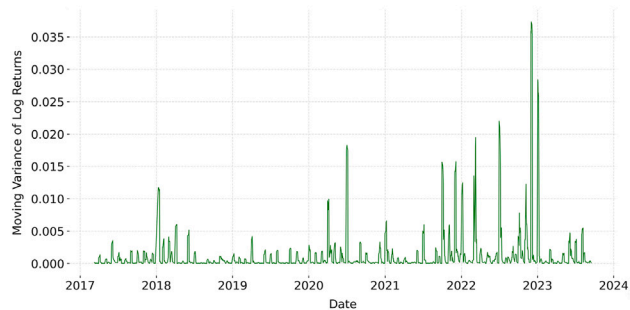
Declaration of competing interest

The authors declare that they have no known competing financial interests or personal relationships that could have appeared to influence the work reported in this paper.

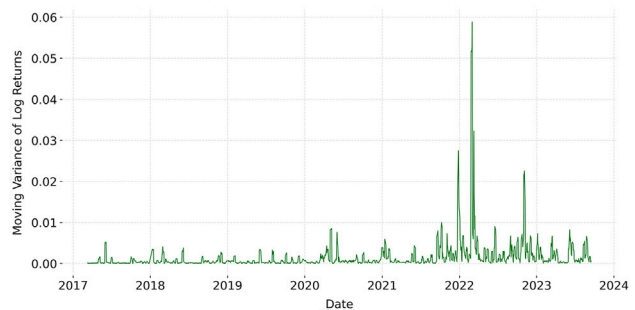
Appendix A

A.1. Behavior of the log-returns moving variance at each maturity

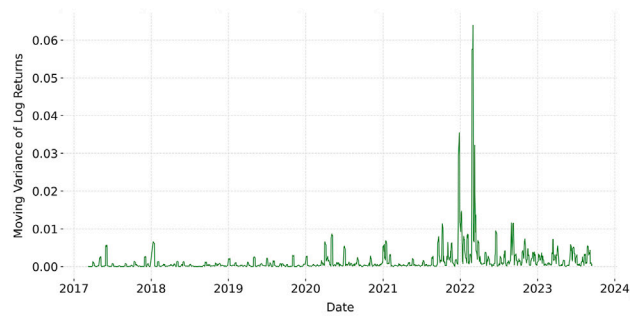
See [Appendix A.14](#).



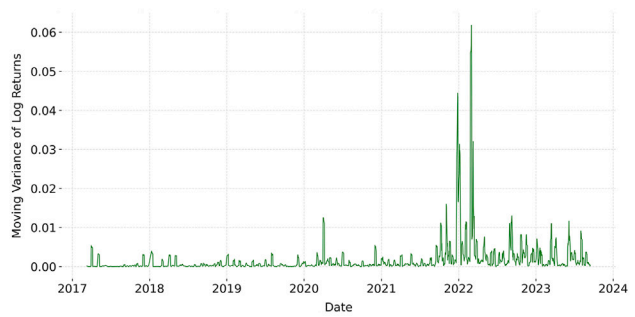
(a)



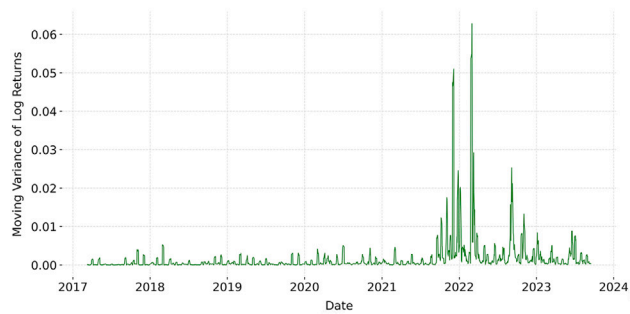
(b)



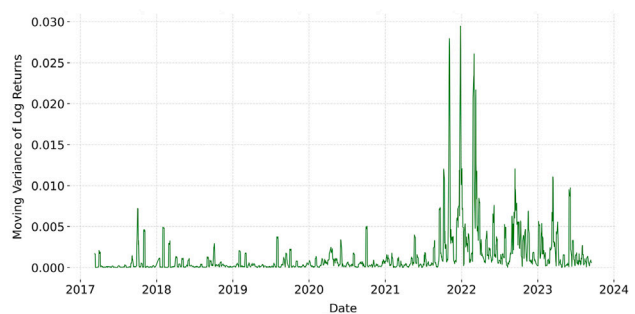
(c)



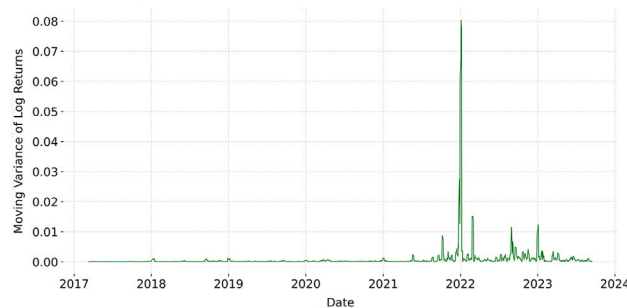
(d)



(e)



(f)



(g)

Fig. A.14. Moving variance (five days window) of the log-returns on the Ec1 (a), Ec2 (b), Ec3 (c), Ec4 (d), Ec5 (e), Ec6 (f) and Ec12 (g) futures contracts.

A.2. Plot of electricity futures prices at each maturity along with the related exogenous variables

See Appendix A.15.

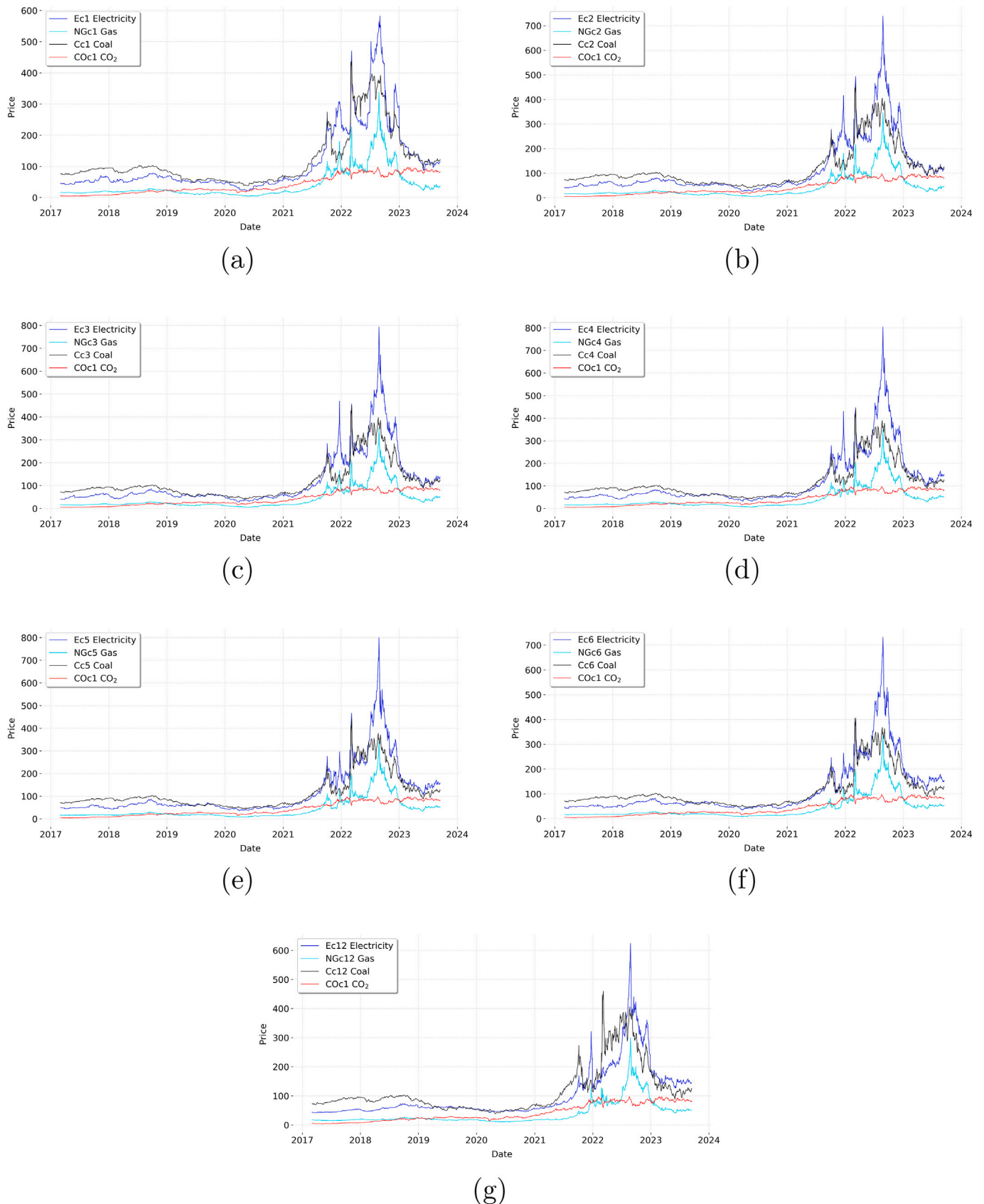


Fig. A.15. Time series of Electricity (dark blue), Natural Gas (light blue), Coal (black) futures prices and Carbon Certificate Emissions (CO₂) spot prices (red). The related maturities are indicated in each plots legend.

Data availability

The authors do not have permission to share data.

References

- [1] Abdulsalam KA, Babatunde OM. Electrical energy demand forecasting model using artificial neural network: a case study of Lagos State Nigeria. *Int J Data Netw Sci* 2019;3:305–22. <https://doi.org/10.5267/j.ijdns.2019.5.002>
- [2] Al-Askar H, Radi N, MacDermott A. Chapter 7 - Recurrent neural networks in medical Data analysis and classifications. In Al-Jumeily D; Hussain A; Mallucci C, Oliver C, editors. *Applied computing in medicine and health. Emerging topics in computer science and applied computing*. Boston: Morgan Kaufmann; 2016. p. 147–65. <https://doi.org/10.1016/B978-0-12-803468-2.00007-2>
- [3] Alasseur C, Féron O. Structural price model for coupled electricity markets. *Energy Econ* 2018;75:104–19. <https://doi.org/10.1016/j.eneco.2018.07.018>
- [4] Aliberti A, Pupillo I, Terna S, Macii E, Di Cataldo S, Patti E, et al. A multi-patient Data-driven approach to blood glucose prediction. *IEEE Access* 2019;7:69311–25. <https://doi.org/10.1109/ACCESS.2019.2919184>
- [5] Almosova A, Andresen N. Nonlinear inflation forecasting with recurrent neural networks. *J Forecast* 2023;42:240–59. <https://doi.org/10.1002/for.2901>. <https://onlinelibrary.wiley.com/doi/abs/10.1002/for.2901>.
- [6] Althelaya KA, El-Alfy E, Mohammed S. Stock market forecast using multivariate analysis with bidirectional and stacked (LSTM, GRU). In: 2018 21st Saudi Computer Society National Computer Conference (NCC); 2018. p. 1–7. <https://doi.org/10.1109/NCC.2018.8593076>
- [7] Apergis N, Gozgor G, Lau C, Wang S. Decoding the Australian electricity market: new evidence from three-regime hidden semi-Markov model. *Energy Econ* 2019;78:129–42. <https://doi.org/10.1016/j.eneco.2018.10.038>
- [8] Arnold F, Çam E, Gruber K, Junkermann J, Kienscherf P. Energy crisis 2022: gas price drives electricity price to record levels. Technical report. Institute of Energy Economics at the University of Cologne; 2022. <https://www.ewi.uni-koeln.de/en/aktuelles/mo-tool-2022-update/#:~:text=Overall,thehigherpricesfor,these-calledmeritorder>
- [9] Aziz N, Abdullah M, Zaidi A. Predictive analytics for crude oil price using RNN-LSTM neural network. In: 2020 International Conference on Computational Intelligence (ICCI); 2020. p. 173–78. <https://doi.org/10.1109/ICCI51257.2020.9247665>
- [10] Barkan O, Benchimol J, Caspi I, Cohen E, Hammer A, Koenigstein N. Forecasting CPI inflation components with hierarchical recurrent neural networks. *Int J Forecast* 2023;39:1145–62. <https://doi.org/10.1016/j.ijforecast.2022.04.009>
- [11] Barth A, Benth F. The forward dynamics in energy markets – infinite-dimensional modelling and simulation. *Stochastics* 2014;86:932–66. <https://doi.org/10.1080/17442508.2014.895359>
- [12] Belenguer E, Segarra-Tamarit J, Pérez E, Vidal-Albalade R. Short-term electricity price forecasting through demand and renewable generation prediction. *Math Comput Simulat* 2025;229:350–61. <https://doi.org/10.1016/j.matcom.2024.10.004>
- [13] Benth F, Koekebakker S. Stochastic modeling of financial electricity contracts. *Energy Econ* 2008;30:1116–57. <https://doi.org/10.1016/j.eneco.2007.06.005>
- [14] Benth F, Krühner P. Spot models and forward pricing. Cham: Springer International Publishing; 2023. p. 111–41 [chapter 5]. https://doi.org/10.1007/978-3-031-40367-5_5
- [15] Biagini F, Bregman J, Meyer-Brandis T. Electricity futures price modeling with Lévy term structure models. *Int J Theor Appl Finance* 2015;18:1550003. <https://doi.org/10.1142/S0219021902491550003X>
- [16] Billé A, Gianfreda A, Del Grosso F, Ravazzolo F. Forecasting electricity prices with expert, linear, and nonlinear models. *Int J Forecast* 2023;39:570–86. <https://doi.org/10.1016/j.ijforecast.2022.01.003>
- [17] Binoy S, Jos J. Financial market forecasting using macro-economic variables and RNN. In: 2022 2nd international conference on Advance Computing and Innovative Technologies in Engineering (ICACITE); 2022. p. 1366–71. <https://doi.org/10.1109/ICACITE53722.2022.9823905>
- [18] Borovkova S, Schmeck M. Electricity price modeling with stochastic time change. *Energy Econ* 2017;63:51–65. <https://doi.org/10.1016/j.eneco.2017.01.002>
- [19] Box GEP, Jenkins GM, Bacon D. Models for forecasting seasonal and non-seasonal time series (stochastic models for forecasting seasonal and nonseasonal time series using iterative method). 1967.
- [20] Brownlee J. Deep Learning for time sEries forecasting: predict the future with MLPs, CNNs and LSTMs in Python. *Machine Learning Mastery*; 2018. <https://books.google.it/books?id=o5qnDwAAQBAJ>
- [21] Bégin JF, Gómez F, Ignatieva K, Li H. The stochastic behavior of electricity prices under scrutiny: evidence from spot and futures markets. *Energy Econ* 2025;144:108296. <https://doi.org/10.1016/j.eneco.2025.108296>
- [22] Callegaro G, Mazzoran A, Sgarra C. A self-exciting modeling framework for forward prices in power markets. *Appl Stochastic Models Bus Ind* 2022;38:27–48. <https://doi.org/10.1002/asmb.2645>
- [23] Chai S, Li Q, Abedin MZ, Lucey BM. Forecasting electricity prices from the state-of-the-art modeling technology and the price determinant perspectives. *Res Int Bus Finance* 2024;67:102132. <https://doi.org/10.1016/j.ribaf.2023.102132>
- [24] Chen Z, Zhang B, Du C, Yang C, Gui W. Outlier-adaptive-based non-crossing quantiles method for day-ahead electricity price forecasting. *Appl Energy* 2025;382:125328. <https://doi.org/10.1016/j.apenergy.2025.125328>
- [25] Cheng H, Ding X, Zhou W, Ding R. A hybrid electricity price forecasting model with Bayesian optimization for German energy exchange. *Int J Electr Power Energy Syst* 2019;110:653–66. <https://doi.org/10.1016/j.ijepes.2019.03.056>
- [26] Chollet F. Keras. 2015. <https://keras.io>
- [27] Coulon M, Howison S. Stochastic behavior of the electricity bid stack: from fundamental drivers to power prices. *J Energy Markets* 2009;2:29–69.
- [28] Dahl GE, Yu D, Deng L, Acero A. Context-dependent pre-trained deep neural networks for large-vocabulary speech recognition. *IEEE Trans Audio Speech Lang Processing* 2012;20:30–42. <https://doi.org/10.1109/TASL.2011.2134090>
- [29] Daneshvar A, Ebrahimi M, Salahi F, Rahmaty M, Homayounfar M. Brent crude oil price Forecast utilizing deep neural network. *Comput Intel Neurosci* 2022. <https://doi.org/10.1155/2022/6140796>
- [30] de Castro Matias M, Tabak B. Comparison of indicator saturation and Markov regime-switching models for Brazilian electricity prices. *Energy Econ* 2025:108341. <https://doi.org/10.1016/j.eneco.2025.108341>
- [31] Deng J, Song W, Zio E. A discrete increment model for electricity price forecasting based on fractional Brownian motion. *IEEE Access* 2020;8:130762–70. <https://doi.org/10.1109/ACCESS.2020.3008797>
- [32] Deschatre T, Féron O, Gruet P. A survey of electricity spot and futures price models for risk management applications. *Energy Econ* 2021;102:105504. <https://doi.org/10.1016/j.eneco.2021.105504>
- [33] Dhamodharavadhani S, Rathipriya R. Dengue incidence rate prediction using non-linear autoregressive neural network time series model. *John Wiley & Sons, Ltd*; 2022. p. 47–68 [chapter 3]. <https://doi.org/10.1002/9781119819165.ch3>
- [34] Di-Giorgi G, Salas R, Avaria R, Ubal C, Rosas H, Torres R. Volatility forecasting using deep recurrent neural networks as GARCH models. *Comput Stat* 2023. <https://doi.org/10.1007/s00180-023-01349-1>
- [35] Dillig M, Jung M, Karl J. The impact of renewables on electricity prices in Germany – an estimation based on historic spot prices in the years 2011–2013. *Renew Sustain Energy Rev* 2016;57:7–15. <https://doi.org/10.1016/j.rser.2015.12.003>
- [36] Drucker H, Burges CJC, Kaufman L, Smola A, Vapnik V. Support vector regression machines. In: Mozer M; Jordan M, Petsche T, editors. *Advances in neural information processing systems*. MIT Press; 1996. https://proceedings.neurips.cc/paper_files/paper/1996/file/d38901788e533e8286cb6400b40b386d-Paper.pdf
- [37] Ehsani B, Pineau PO, Charlin L. Price forecasting in the Ontario electricity market via TriConvGRU hybrid model: univariate vs. multivariate frameworks. *Appl Energy* 2024;359:122649. <https://doi.org/10.1016/j.apenergy.2024.122649>
- [38] Electricity Authority Te Mana Hiko. The forward electricity market explained. Technical Report. Electricity Authority Te Mana Hiko; 2022. <https://www.ea.govt.nz/news/eye-on-electricity/the-forward-electricity-market-explained/>
- [39] Fanelli V, Maddalena L, Musti S. Modelling electricity futures prices using seasonal path-dependent volatility. *Appl Energy* 2016;173:92–102. <https://doi.org/10.1016/j.apenergy.2016.04.003>
- [40] Féron O, Gruet P. Estimation of the number of factors in a multi-factorial heath-jarrow-morton model in power markets. Cham: Springer Nature Switzerland; 2024. p. 3–39 [chapter Part 1]. https://doi.org/10.1007/978-3-031-50597-3_1
- [41] Fontcuberta AE, Ghosh A, Chatterjee S, Mitra D, Nandy D. Forecasting solar cycle 25 with physical model-validated recurrent neural networks. *Sol Phys* 2023;298. <https://doi.org/10.1007/s11207-022-02104-3>
- [42] Frydenberg S, Onochie JJ, Westgaard S, Midtsund N, Ueland H. Long-term relationships between electricity and oil, gas and coal future prices—evidence from Nordic countries, Continental Europe and the United Kingdom. *OPEC Energy Rev* 2014;38:216–42. <https://doi.org/10.1111/opeec.12025>
- [43] Füss R, Mahringer S, Prokopczuk M. Electricity derivatives pricing with forward-looking information. *J Econ Dyn Control* 2015;58:34–57. <https://doi.org/10.1016/j.jedc.2015.05.016>
- [44] Gardini M, Santilli E. A Heath–Jarrow–Morton framework for energy markets: review and applications for practitioners. *Decis Econ Finance* 2024. <https://doi.org/10.1007/s10203-024-00484-8>
- [45] Ghosh S, Bohra A, Dutta S. The Texas freeze of February 2021: event and winterization analysis using cost and pricing data. In: 2021 IEEE electrical power and energy conference (EPEC); 2021. p. 7–13. <https://doi.org/10.1109/EPEC52095.2021.9621500>
- [46] Gonzalez V, Contreras J, Bunn D. Forecasting Power prices using a hybrid fundamental-econometric model. *IEEE Trans Power Syst* 2012;27:363–72. <https://doi.org/10.1109/TPWRS.2011.2167689>
- [47] Graves A, Rahman Mohamed A, Hinton G. Speech recognition with deep recurrent neural networks. In: 2013 IEEE international conference on Acoustics, Speech and Signal Processing; 2013. p. 6645–49. <https://doi.org/10.1109/ICASSP.2013.6638947>
- [48] Graves A, Schmidhuber J. Framewise phoneme classification with bidirectional LSTM networks. In: Proceedings. 2005 IEEE international joint conference on neural networks, 2005, vol. 4; 2005. p. 2047–52. <https://doi.org/10.1109/IJCNN.2005.1556215>
- [49] Gudkov N, Ignatieva K. Electricity price modelling with stochastic volatility and jumps: an empirical investigation. *Energy Econ* 2021;98:105260. <https://doi.org/10.1016/j.eneco.2021.105260>
- [50] Harvey D, Leybourne S, Newbold P. Testing the equality of prediction mean squared errors. *Int J Forecast* 1997;13:281–91. [https://doi.org/10.1016/S0169-2070\(96\)00719-4](https://doi.org/10.1016/S0169-2070(96)00719-4)
- [51] Higgs H, Worthington A. Stochastic price modeling of high volatility, mean-reverting, spike-prone commodities: the Australian wholesale spot electricity market. *Energy Econ* 2008;30:3172–85 [Technological change and the environment]. <https://doi.org/10.1016/j.eneco.2008.04.006>
- [52] Hochreiter S, Schmidhuber J. Long short-term memory. *Neural Comput* 1997;9:1735–80. <https://doi.org/10.1162/NECO.1997.9.8.1735>
- [53] Hornik K, Stinchcombe M, White H. Multilayer feedforward networks are universal approximators. *Neural Netw* 1989;2:359–66. [https://doi.org/10.1016/0893-6080\(89\)90020-8](https://doi.org/10.1016/0893-6080(89)90020-8)

- [54] Hultén E, Wahde M. Improved time series prediction using evolutionary algorithms for the generation of feedback connections in neural networks, vol. 38. WIT Press; 2004. p. 211–219 [chapter 20]. <https://doi.org/10.2495/CF040201>
- [55] Islyayev S, Date P. Electricity futures price models: calibration and forecasting. *Eur J Oper Res* 2015;247:144–54. <https://doi.org/10.1016/j.ejor.2015.05.063>
- [56] Ivakhnenko AG, Lapa VG. Cybernetic predicting devices. CCM Information Corporation; 1965.
- [57] Jahangir H, Tayarani H, Baghali S, Ahmadian A, Elkamel A, Golkar M, et al. A novel electricity price forecasting approach based on dimension reduction strategy and rough artificial neural networks. *IEEE Trans Ind Inf* 2020;16:2369–81. <https://doi.org/10.1109/TII.2019.2933009>
- [58] Jiang H, Pan S, Dong Y, Wang J. Probabilistic electricity price forecasting based on penalized temporal fusion transformer. *J Forecast* 2024;43:1465–91. <https://doi.org/10.1002/for.3084>
- [59] Jones D, Brown S, Czyżak P. European electricity review 2023. Technical Report. EMBER; 2023. <https://ember-climate.org/insights/research/european-electricity-review-2023/>
- [60] Kallabis T, Pape C, Weber C. The plunge in German electricity futures prices – analysis using a parsimonious fundamental model. *Energy Policy* 2016;95:280–90. <https://doi.org/10.1016/j.enpol.2016.04.025>
- [61] Kanamura T, Bunn D. Market making and electricity price formation in Japan. *Energy Econ* 2022;107:105765. <https://doi.org/10.1016/j.eneco.2021.105765>
- [62] Karakatsani N, Bunn D. Forecasting electricity prices: the impact of fundamentals and time-varying coefficients. *Int J Forecast* 2008;24:764–85 [Energy Forecasting]. <https://doi.org/10.1016/j.ijforecast.2008.09.008>
- [63] Kavitha G, Kalpana K. Integrated tuning of hidden Markov parametric optimization model with genetic algorithm for electricity market forecasting. In: Silhavy R, Silhavy P, Prokopova Z, editors. *Data science and algorithms in systems*; Cham: Springer International Publishing; 2023. p. 798–806.
- [64] Khudoley K. New Russia-West confrontation: war of attrition or escalation? *Strateg Anal* 2022;46:571–84. <https://doi.org/10.1080/09700161.2022.2149980>
- [65] Kiesel R, Paraschiv F, Sætherø A. On the construction of hourly price forward curves for electricity prices. *Comput Manag Sci* 2019;16:345–69. <https://doi.org/10.1007/s10287-018-0300-6>
- [66] Kim W, Jung G, Choi S. Forecasting CDS term structure based on Nelson-Siegel model and machine learning. *Complexity* 2020;2020:2518283:1–2518283:23.
- [67] Kingma DP, Ba J. Adam: a method for stochastic optimization. In: Bengio Y, LeCun Y, editors. *3rd international conference on learning representations, ICLR 2015, San Diego, CA, USA, May 7–9, 2015, Conference track proceedings*; 2015. <http://arxiv.org/abs/1412.6980>
- [68] Ko MS, Lee K, Kim JK, Hong CW, Dong ZY, Hur K. Deep concatenated residual network with bidirectional LSTM for one-hour-ahead wind power forecasting. *IEEE Trans Sustain Energy* 2021;12:1321–35. <https://doi.org/10.1109/TSTE.2020.3043884>
- [69] Koekebakker S, Ollmar F. Forward curve dynamics in the Nordic electricity market. *Manage Financ* 2005;31:73–94. <https://doi.org/10.1108/03074350510769703>
- [70] Kostrzewski M, Kostrzewska J. Probabilistic electricity price forecasting with Bayesian stochastic volatility models. *Energy Econ* 2019;80:610–20. <https://doi.org/10.1016/j.eneco.2019.02.004>
- [71] Kumar R, Kumar P, Kumar Y. Analysis of Financial time series forecasting using deep learning model. In: *2021 11th international conference on cloud computing, data science & engineering (Confluence)*; 2021. p. 877–81. <https://doi.org/10.1109/Confluence51648.2021.9377158>
- [72] Kumar V, Singh N, Singh D, Mohanty S. Short-term electricity price forecasting using hybrid SARIMA and GJR-GARCH model. In: Perez G, Mishra K, Tiwari S, Trivedi M, editors. *Networking Communication and Data Knowledge Engineering*; Singapore: Springer Singapore; 2018. p. 299–310.
- [73] Kuo P, Huang C. An electricity price forecasting model by hybrid structured deep neural networks. *Sustainability* 2018;10. <https://doi.org/10.3390/su10041280>
- [74] Lago J, Marcjasz G, De Schutter B, Weron R. Forecasting day-ahead electricity prices: a review of state-of-the-art algorithms, best practices and an open-access benchmark. *Appl Energy* 2021;293:116983. <https://doi.org/10.1016/j.apenergy.2021.116983>
- [75] Larochelle H, Bengio Y, Louradour J, Lamblin P. Exploring strategies for training deep neural networks. *Journal Of Machine Learning Research* 2009;10:1–40. <http://jmlr.org/papers/v10/larochelle09a.html>
- [76] Lehna M, Scheller F, Herwartz H. Forecasting day-ahead electricity prices: a comparison of time series and neural network models taking external regressors into account. *Energy Econ* 2022;106:105742. <https://doi.org/10.1016/j.eneco.2021.105742>
- [77] Levenberg K. A method for the solution of certain non-linear problems in least squares. *Q Appl Math* 1944;2:164–68. <http://www.jstor.org/stable/43633451>
- [78] Liu E, Zhu H, Liu Q, Udimal T. Regional economic forecasting method based on recurrent neural network. *Math Probl Eng* 2022. <https://doi.org/10.1155/2022/3058947>
- [79] Ljung L. System identification: theory for the user. Prentice Hall information and system sciences series. Prentice Hall PTR; 1999. <https://books.google.it/books?id=nHfoQgAACAAJ>
- [80] Longo L, Riccaboni M, Rungi A. A neural network ensemble approach for GDP forecasting. *J Econ Dyn Control* 2022;134:104278. <https://doi.org/10.1016/j.jedc.2021.104278>
- [81] Lu M, Xu X. TRNN: an efficient time-series recurrent neural network for stock price prediction. *Inf Sci (NY)* 2024;657:119951. <https://doi.org/10.1016/j.ins.2023.119951>
- [82] Machalek D, Tuttle J, Andersson K, Powell KM. Dynamic energy system modeling using hybrid physics-based and machine learning encoder–decoder models. *Energy AI* 2022;9:100172. <https://doi.org/10.1016/j.egyai.2022.100172>
- [83] Maciejowska K, Nitka W, Weron T. Enhancing load, wind and solar generation for day-ahead forecasting of electricity prices. *Energy Econ* 2021;99:105273. <https://doi.org/10.1016/j.eneco.2021.105273>
- [84] Mao X, Chen S, Yu H, Duan L, He Y, Chu Y. Simplicity in dynamic and competitive electricity markets: a case study on enhanced linear models versus complex deep-learning models for day-ahead electricity price forecasting. *Appl Energy* 2025;383:125201. <https://doi.org/10.1016/j.apenergy.2024.125201>
- [85] Marquardt D. An algorithm for least-squares estimation of nonlinear parameters. *SIAM J Appl Math* 1963;11:431–41. <https://www.jstor.org/stable/2098941>
- [86] Mehrdoust F, Noorani I. Forward price and fitting of electricity Nord Pool market under regime-switching two-factor model. *Math Financ Econ* 2021;15:501–43. <https://doi.org/10.1007/s11579-020-00287-6>
- [87] Mehrdoust F, Noorani I, Xu W. Uncertain energy model for electricity and gas futures with application in spark-spread option price. *Fuzzy Optim Dec Making* 2023;22:123–48. <https://doi.org/10.1007/s10700-022-09386-z>
- [88] Men L, Ilk N, Tang X, Liu Y. Multi-disease prediction using LSTM recurrent neural networks. *Expert Syst Appl* 2021;177:114905. <https://doi.org/10.1016/j.eswa.2021.114905>
- [89] Mishura Y, Ottaviano S, Vargiolu T. Gaussian volta processes as models of electricity markets. *SIAM J Financ Math* 2024;15:989–1019. <https://doi.org/10.1137/23M1617370>
- [90] Moghar A, Hamiche M. Stock market prediction using LSTM recurrent neural network. *Procedia Comput Sci* 2020;170:1168–73. <https://doi.org/10.1016/j.procs.2020.03.049>
- [91] Monjaze M, Amiri H, Movahedi A. Wholesale electricity price forecasting by quantile regression and kalman filter method. *Energy* 2024;290:129925. <https://doi.org/10.1016/j.energy.2023.129925>
- [92] Mosquera-López S, Nursimulu A. Drivers of electricity price dynamics: comparative analysis of spot and futures markets. *Energy Policy* 2019;126:76–87. <https://doi.org/10.1016/j.enpol.2018.11.020>
- [93] Mubarak H, Abdellatif A, Ahmad S, Zohurul Islam M, Muyeen S, Abdul Mannan M, et al. Day-ahead electricity price forecasting using a CNN-BiLSTM model in conjunction with autoregressive modeling and hyperparameter optimization. *Int J Electr Power Energy Syst* 2024;161:110206. <https://doi.org/10.1016/j.ijepes.2024.110206>
- [94] Mulla S, Pande CB, Singh SK. Times series forecasting of monthly rainfall using seasonal auto regressive integrated moving average with exogenous variables (SARIMAX) model. *Water Resour Manage* 2024;38:1825–46. <https://doi.org/10.1007/s11269-024-03756-5>
- [95] Najafi A, Taleghani R, Mehrdoust F. Forward contract prices of electricity Nord Pool market: calibration and jump approximation. *Sādhanā* 2023;48:11–48. <https://doi.org/10.1007/s12046-022-02056-1>
- [96] Nascimento J, Pinto T, Vale Z. Electricity price forecast for futures contracts with artificial neural network and spearman data correlation. In: *Distributed computing and artificial intelligence, special sessions, 15th international conference*; Cham: Springer International Publishing; 2019. p. 12–20. https://doi.org/10.1007/978-3-319-99608-0_2
- [97] Nguyen HT, Nguyen DT. Transfer learning for macroeconomic forecasting. In: *2020 7th NAFOSTED conference on information and computer science (NICS)*; 2020. p. 332–37. <https://doi.org/10.1109/NICSS1282.2020.9335848>
- [98] Nickelsen D, Müller G. Bayesian hierarchical probabilistic forecasting of intra-day electricity prices. *Appl Energy* 2025;380:124975. <https://doi.org/10.1016/j.apenergy.2024.124975>
- [99] Nowotarski J, Weron R. Recent advances in electricity price forecasting: a review of probabilistic forecasting. *Renew Sustain Energy Rev* 2018;81:1548–68. <https://doi.org/10.1016/j.rser.2017.05.234>
- [100] Oduor D. Mean: reverting logistic Brownian motion with jump diffusion process on energy commodity prices. *Int J Stat Appl Math* 2022;7:69–74.
- [101] Olivares K, Challu C, Marcjasz G, Weron R, Dubrawski A. Neural basis expansion analysis with exogenous variables: forecasting electricity prices with NBEATSx. *Int J Forecast* 2022. <https://doi.org/10.1016/j.ijforecast.2022.03.001>
- [102] Paschalidou EG, Thomaidis NS. Risk factors in the formulation of day-ahead electricity prices: evidence from the Spanish case. *Energy Econ* 2025;142:108102. <https://doi.org/10.1016/j.eneco.2024.108102>
- [103] Pedregosa F, Varoquaux G, Gramfort A, Michel V, Thirion B, Grisel O, et al. Scikit-learn: machine learning in Python. *J Mach Learn Res* 2011;12:2825–30. <https://www.jmlr.org/papers/v12/pedregosa11a.html>
- [104] Peng L, Liu S, Liu R, Wang L. Effective long short-term memory with differential evolution algorithm for electricity price prediction. *Energy* 2018;162:1301–14. <https://doi.org/10.1016/j.energy.2018.05.052>
- [105] Pircalabu A, Benth F. A regime-switching copula approach to modeling day-ahead prices in coupled electricity markets. *Energy Econ* 2017;68:283–302. <https://doi.org/10.1016/j.eneco.2017.10.008>
- [106] Potdar K, Kinnerkar R. A non-linear autoregressive neural network model for forecasting Indian index of industrial production. In: *2017 IEEE region 10 symposium (TENSYMP)*; 2017. p. 1–5. <https://doi.org/10.1109/TENCONSpring.2017.8069973>
- [107] Pourdayaei A, Mohammadi M, Mubarak H, Abdellatif A, Karimi M, Gryzina E, et al. A new framework for electricity price forecasting via multi-head self-attention and CNN-based techniques in the competitive electricity market. *Expert Syst Appl* 2024;235:121207. <https://doi.org/10.1016/j.eswa.2023.121207>

- [108] Povh M, Fleten SE. Modeling long-term electricity forward prices. *IEEE Trans Power Syst* 2009;24:1649–56. <https://doi.org/10.1109/TPWRS.2009.2030285>
- [109] Pustokhina I, Pustokhin D, Gupta D, Khanna A, Shankar K, Nguyen G. An effective training scheme for deep neural network in edge computing enabled internet of medical things (IoMT) systems. *IEEE Access* 2020;8:107112–23. <https://doi.org/10.1109/ACCESS.2020.3000322>
- [110] Rafiei M, Niknam T, Khooban M. Probabilistic electricity price forecasting by improved clonal selection algorithm and wavelet preprocessing. *Neural Comput Appl* 2017;28:3889–901. <https://doi.org/10.1007/s00521-016-2279-7>
- [111] Ramirez M, Melin P. Modular perspective for population and gross national income time series prediction using a neural network model: a case study of OECD member countries. Cham: Springer Nature Switzerland; 2024. p. 63–71 [chapter 6]. https://doi.org/10.1007/978-3-031-53713-4_6
- [112] Raviv E, Bouwman KE, van Dijk D. Forecasting day-ahead electricity prices: utilizing hourly prices. *Energy Econ* 2015;50:227–39. <https://doi.org/10.1016/j.eneco.2015.05.014>
- [113] Ribeiro M, Stefenon S, de Lima J, Nied A, Mariani V, Coelho L. Electricity price forecasting based on self-adaptive decomposition and heterogeneous ensemble learning. *Energies* 2020;13. <https://doi.org/10.3390/en13195190>
- [114] Rumelhart D, Hinton G, Williams R. Learning representations by back-propagating errors. *Nature* 1986;323:533–36. <https://doi.org/10.1038/323533a0>
- [115] Samarawickrama A, Fernando T. A recurrent neural network approach in predicting daily stock prices an application to the Sri Lankan stock market. In: 2017 IEEE international conference on industrial and information systems (ICIIS); 2017. p. 1–6. <https://doi.org/10.1109/ICIINFS.2017.8300345>
- [116] Sapnken F, Khalili Tazehkandgheshlagh A, Salomon Diboma B, Hamaidi M, Gopdjim Noumo P, Wang Y, et al. A whale optimization algorithm-based multivariate exponential smoothing grey-holt model for electricity price forecasting. *Expert Syst Appl* 2024;255:124663. <https://doi.org/10.1016/j.eswa.2024.124663>
- [117] Schuster M, Paliwal KK. Bidirectional recurrent neural networks. *IEEE Trans Signal Process* 1997;45:2673–81. <https://doi.org/10.1109/78.650093>
- [118] Shen ML, Lee CF, Liu HH, Chang PY, Yang CH. Effective multinational trade forecasting using LSTM recurrent neural network. *Expert Syst Appl* 2021;182:115199. <https://doi.org/10.1016/j.eswa.2021.115199>
- [119] Siddiqui A. Predicting natural gas spot prices using artificial neural network. In: 2019 2nd international conference on computer applications & information security (ICCAIS); 2019. p. 1–6. <https://doi.org/10.1109/CAIS.2019.8769586>
- [120] da Silva P, Horta P. The effect of variable renewable energy sources on electricity price volatility: the case of the Iberian market. *Int J Sustain Energy* 2019;38:794–813. <https://doi.org/10.1080/14786451.2019.1602126>
- [121] Su H, Peng X, Liu H, Quan H, Wu K, Chen Z. Multi-step-ahead electricity price forecasting based on temporal graph convolutional network. *Mathematics* 2022;10. <https://doi.org/10.3390/math10142366>
- [122] Sutskever I, Vinyals O, Le Q. Sequence to sequence learning with neural networks. In: Ghahramani Z, Welling M; Cortes C; Lawrence N, Weinberger K, editors. *Advances in neural information processing systems*; Curran Associates, Inc.; 2014.
- [123] Syed F, Sipio RD, Sinervo P. Bidirectional long short-term memory (BLSTM) neural networks for reconstruction of top-quark pair decay kinematics. *arXiv preprint* 2019. [arXiv:1909.01144](https://arxiv.org/abs/1909.01144).
- [124] Szandala T. Review and comparison of commonly used activation functions for deep neural networks. Singapore: Springer Singapore; 2021. p. 203–24. https://doi.org/10.1007/978-981-15-5495-7_11
- [125] Tan Z, Zhang J, Wang J, Xu J. Day-ahead electricity price forecasting using wavelet transform combined with ARIMA and GARCH models. *Appl Energy* 2010;87:3606–10. <https://doi.org/10.1016/j.apenergy.2010.05.012>
- [126] Tölö E. Predicting systemic financial crises with recurrent neural networks. *J Financ Stabil* 2020;49:100746. <https://doi.org/10.1016/j.jfs.2020.100746>
- [127] Tschora L, Pierre E, Plantevit M, Robardet C. Electricity price forecasting on the day-ahead market using machine learning. *Appl Energy* 2022;313:118752. <https://doi.org/10.1016/j.apenergy.2022.118752>
- [128] Tselika K, Tselika M, Demetriades E. Quantifying the short-term asymmetric effects of renewable energy on the electricity merit-order curve. *Energy Econ* 2024;132:107471. <https://doi.org/10.1016/j.eneco.2024.107471>
- [129] Uribe JM, Mosquera-López S, Arenas OJ. Assessing the relationship between electricity and natural gas prices in European markets in times of distress. *Energy Policy* 2022;166:113018. <https://doi.org/10.1016/j.enpol.2022.113018>
- [130] Vida K, Bódi A, Szklenár T, Seli B. Finding flares in Kepler and TESS data with recurrent deep neural networks. *Astron Astrophys* 2021;652:A107. <https://doi.org/10.1051/0004-6361/202141068>
- [131] Voronin S, Partanen J, Kauranne T. A hybrid electricity price forecasting model for the Nordic electricity spot market. *Int Trans Electr Energy Syst* 2013;24:736–60. <https://doi.org/10.1002/etep.1734>
- [132] Wang B, Wang J. Energy futures price prediction and evaluation model with deep bidirectional gated recurrent unit neural network and RIF-based algorithm. *Energy* 2021;216:119299. <https://doi.org/10.1016/j.energy.2020.119299>
- [133] Wang F, Xuan Z, Zhen Z, Li K, Wang T, Shi M. A day-ahead PV power forecasting method based on LSTM-RNN model and time correlation modification under partial daily pattern prediction framework. *Energy Convers Manag* 2020;212:112766. <https://doi.org/10.1016/j.enconman.2020.112766>
- [134] Wang Y, Qin L, Wang Q, Chen Y, Yang Q, Xing L, et al. A novel deep learning carbon price short-term prediction model with dual-stage attention mechanism. *Appl Energy* 2023;347:121380. <https://doi.org/10.1016/j.apenergy.2023.121380>
- [135] Weron R. Electricity price forecasting: a review of the state-of-the-art with a look into the future. *Int J Forecast* 2014;30:1030–81. <https://doi.org/10.1016/j.ijforecast.2014.08.008>
- [136] Wiczorek M, Siłka J, Woźniak M. Neural network powered COVID-19 spread forecasting model. *Chaos Solitons Fractals* 2020;140:110203. <https://doi.org/10.1016/j.chaos.2020.110203>
- [137] Willamowski B, Irwin J, editors. *Intelligent systems*. 2nd ed. CRC Press; 2011. <https://doi.org/10.1201/9781315218427>
- [138] Wilkens S, Wimschulte J. The pricing of electricity futures: evidence from the European energy exchange. *J Futures Markets* 2007;27:387–410. <https://doi.org/10.1002/fut.20246>
- [139] Xiong H, Mamon R. A higher-order Markov chain-modulated model for electricity spot-price dynamics. *Appl Energy* 2019;233-234:495–515. <https://doi.org/10.1016/j.apenergy.2018.09.039>
- [140] Xu X, Zhang Y. Neural network predictions of the high-frequency CSI300 first distant futures trading volume. *Financ Mark Portf Mang* 2023;37:191–207. <https://doi.org/10.1007/s11408-022-00421-y>
- [141] Yang B, He B, Wan J, Kubal S, Zhao Y. Applications of neural networks to dynamics simulation of Landau-Zener transitions. *Chem Phys* 2020;528:110509. <https://doi.org/10.1016/j.chemphys.2019.110509>
- [142] Yang H, Schell KR. Real-time electricity price forecasting of wind farms with deep neural network transfer learning and hybrid datasets. *Appl Energy* 2021;299:117242. <https://doi.org/10.1016/j.apenergy.2021.117242>
- [143] Yang W, Wang J, Niu T, Du P. A novel system for multi-step electricity price forecasting for electricity market management. *Appl Soft Comput* 2020;88:106029. <https://doi.org/10.1016/j.asoc.2019.106029>
- [144] Yu J, Zhou L, Xia A. Power futures price forecasting based on improved wavelet neural network. In: 2008 third international conference on electric utility deregulation and restructuring and power technologies; 2008. p. 521–26. <https://doi.org/10.1109/DRPT.2008.4523462>
- [145] Zhang J, Tan Z, Wei Y. An adaptive hybrid model for short term electricity price forecasting. *Appl Energy* 2020;258:114087. <https://doi.org/10.1016/j.apenergy.2019.114087>
- [146] Zhang K, Shi Q. Power futures price forecasting based on RBF neural network. In: 2009 international conference on business intelligence and financial engineering; 2009. p. 50–2. <https://doi.org/10.1109/BIFE.2009.21>
- [147] Zhang R, Li G, Ma Z. A deep learning based hybrid framework for day-ahead electricity price forecasting. *IEEE Access* 2020;8:143423–36. <https://doi.org/10.1109/ACCESS.2020.3014241>
- [148] Zhang X, Wang J, Gao Y. A hybrid short-term electricity price forecasting framework: cuckoo search-based feature selection with singular spectrum analysis and SVM. *Energy Econ* 2019;81:899–913. <https://doi.org/10.1016/j.eneco.2019.05.026>
- [149] Zhao Z, Wang C, Nokleby M, Miller C. Improving short-term electricity price forecasting using day-ahead LMP with ARIMA models. In: 2017 IEEE Power & Energy Society general meeting; 2017. p. 1–5. <https://doi.org/10.1109/PESGM.2017.8274124>
- [150] Zhou F, Huang Z, Zhang C. Carbon price forecasting based on CEEMDAN and LSTM. *Appl Energy* 2022;311:118601. <https://doi.org/10.1016/j.apenergy.2022.118601>
- [151] Zhou S, Zhou L, Mao M, Tai H, Wan Y. An optimized heterogeneous structure LSTM network for electricity price forecasting. *IEEE Access* 2019;7:108161–73. <https://doi.org/10.1109/ACCESS.2019.2932999>
- [152] Ziel F, Steinert R. Probabilistic mid- and long-term electricity price forecasting. *Renew Sustain Energy Rev* 2018;94:251–66. <https://doi.org/10.1016/j.rser.2018.05.038>
- [153] Ziel F, Weron R. Day-ahead electricity price forecasting with high-dimensional structures: univariate vs. multivariate modeling frameworks. *Energy Econ* 2018;70:396–420. <https://doi.org/10.1016/j.eneco.2017.12.016>